MODELLING BIOLOGICAL MACROMOLECULES IN SOLUTION: THE GENERAL TRI-AXIAL ELLIPSOID

Stephen Ernest Harding, M.A. (Oxon), M.Sc.

PhD Dissertation

University of Leicester

1980

CHAPTER 1

The Mass, Size and Shape of Macromolecules in Solution: The Ellipsoid of Revolution Model

1.1. Macromolecular Structure in Solution

The concept of a unique structure for a biological macromolecule in solution and in crystallized form has only relatively recently been established beyond dispute. Prior to the work of Svedberg the view was commonly taken (Sorensen, 1930) that proteins and other macromolecules exist in solution not as unique structures but as dissociable complexes containing possibly several components, that the equilibrium state was dependent on circumstances (for example the composition of the solution) and any components precipitated are not necessarily to be identified with those occurring in solution. Researchers were consequently surprised at the ultracentrifuge results of Svedberg and his co-workers (Svedberg & Pedersen, 1940) which strongly suggested the molecular homogeneity of many protein systems. Thus, in striking contrast to the polydispersity of many polymer systems (such as carbohydrates, rubber or polystyrene) it was deduced that carefully prepared protein solutions contain one, or at the most a few, different molecular species. This deduction was derived mainly from the observation that boundary spreading observed in the sedimentation of protein solutions could be identified with separately measured translational diffusion coefficients. Bresler and Talmud (1944) suggested however that a monodisperse protein really contains a distribution of molecular weights with a sharply defined maximum. This surmise is, on the other hand, strongly opposed by the immunological properties of proteins (Alexander & Johnson, 1949) together with the overwhelming evidence now available from protein crystallography (Kendrew et al, 1958, Perutz et al, 1960, Blake et al, 1965, Feldman, 1976) which support the idea of discrete individual structures.

X-ray crystallography is by far the most accurate method for determining these structures. Unfortunately this technique is also the most laborious, requiring several researchers working for a period of months to determine the structure of a single globular protein. The calculated structures are also of the 'fossilized' form of the macromolecule which may not necessarily be the same in solution. There are many techniques available, such as nuclear magnetic resonance, electron spin resonance, fluorescence and other spectroscopic techniques which can give much detailed information about the dynamic properties of localized regions of macromolecules in solution (for example, the active sites of enzymes are being extensively studied). These techniques cannot however give information as to the overall macromolecular mass, size and shape. For this one needs to consider the hydrodynamic properties of solutions of the macromolecule (although scattering phenomena can also give useful information), which allows determination of the molecular weight, simple 'hydrodynamically equivalent' mathematical models for the structure and also the size (including the swelling due to solvent association) of the macromolecule.

1.1.1. Mass

The 'inertial mass' of a body can be defined as the quantity of matter in it, or as the ratio of the force applied to its acceleration (Newton's 2nd Law of Motion). For a macromolecule we conveniently express the mass by the 'Molecular Weight' (M_r) which is defined as the ratio of the mass of the macromolecule to that of one sixteenth of an oxygen O_{16} atom, and is expressed in grams.

The mass of fluid displaced by a macromolecule in a solution will

equal the product of the volume displaced and the density of the solution $(M_r\bar{v}/N_A)\rho_o$, where M_r is the molecular weight, N_A Avogadro's number, ρ_o the solution density and $\bar{v}$ the partial specific volume of the macromolecule, i.e. the volume increase when unit mass (generally one gram) of solute is added to an infinite volume of the solvent at constant temperature and *pressure*

$$\bar{v} = \left(\frac{\partial v}{\partial m}\right)_{T,p} \qquad (1)$$

The 'Archimedean mass' (i.e. the buoyant mass) of a macromolecule (Van Holde, 1971) in solution will equal the true mass minus the mass of the fluid displaced:

$$= \frac{M_r}{N_A} - \left[\frac{M_r}{N_A}\bar{v}\right]\rho_o = \frac{M_r}{N_A}(1 - \bar{v}\rho_o) \qquad (2)$$

The molecular weight of a macromolecular solute can be measured from many methods, for example sedimentation velocity and translational diffusion, osmosis, light or x-ray scattering, or most precisely from a sequence analysis. A recent review of these methods is given by Rowe (1978). The partial specific volume can be found either from a concentration determination followed by a densimetric analysis (Kratky et al, 1969, 1973), or for a protein, from Traube's rule (Rowe, 1978). This rule may possibly also be applicable to nucleic acids (Pearce et al, 1975).

1.1.2. Size

The size of a rigid macromolecule in solution will differ from that in the anhydrous state because of associated solvent. The hydrodynamic or swollen specific volume $\bar{v}_s$, will now comprise of the partial specific

volume, $\bar{v}$, the bound solvent that adheres to the hydrophilic particle surface, and 'entrained' solvent which may be trapped in the various cavities and indentations in the macromolecule (Figure 1). The ratio $\bar{v}_s / \bar{v}$ is known as the 'swelling' of the macromolecule and is equal to unity if the macromolecule is anhydrous and compact in solution. The swollen specific volume can be simply related to the "effective" hydrodynamic volume V_e i.e. the swollen volume of a single macromolecule in a homogeneous solution:

$$V_e = \frac{\bar{v}_s M_r}{N_A} \qquad (3)$$

1.1.3. Shape

Owing to the difficulties in developing theoretical relationships between the shape of a macromolecule and experimentally measurable parameters, only rather simple 'hydrodynamically equivalent' models are currently available, the boundaries of which can be described by a simple mathematical equation; these are (Figure 2) rods, discs and ellipsoids of revolution (Tanford, 1961).

An ellipsoid of revolution is formed by rotating an ellipse either about the major axis (prolate ellipsoid) or about the minor axis (oblate ellipsoid) and thus has the necessary restriction that two of the three axes must be equal. In the limit of large axial ratio, a prolate ellipsoid (2 minor axes, 1 major) becomes a good approximation to a rod whilst an oblate ellipsoid (2 major axes, 1 minor) becomes a good approximation to a disc. Consequently, physical biochemists have tended to use the ellipsoid of revolution model to determine the hydrodynamically equivalent shape of a rigid macromolecule in solution.

It should be made clear at this stage that many macromolecules cannot be modelled by any of these rigid structures as they have no preferred

structure in solution: these 'randomly coiled' macromolecules can only be represented by probability configurations. Many other macromolecules have a well defined rigid structure but cannot be reasonably modelled, judging from the x-ray models at least, by any ellipsoid. The L-shaped Transfer RNA molecule is an outstanding example (Kim, 1974).

1.2. The Hydrodynamic Properties of a Macromolecular Solution

The hydrodynamic properties of a macromolecular solution, which are used to determine these structures, can be conveniently divided into three broad classes:

(i) The viscosity property, which concerns the effect of the dissolved macromolecule on the bulk motion of the fluid when a shear gradient is applied.

(ii) The translational frictional property, which concerns the movement of the macromolecule through its solution when some form of external force is applied. This can be a centrifugal field in a sedimentation experiment or a concentration gradient (i.e. a gradient of chemical potential) in a translational diffusion experiment.

(iii) The rotational frictional property, which concerns the disorienting effect on the macromolecule by the local Brownian motion of the surrounding solvent molecules.

1.3. The Viscosity Property of a Macromolecular Solution

The viscosity of a fluid is a measure of its resistance to flow and may be simply defined for a simple shearing flow* (Figure 3) in terms of the shearing stress σ and the shear rate G:

$$\sigma = \eta G \qquad (4)$$

---

* For the equations describing a more general flow see Batchelor (1967).

where η is known as the viscosity coefficient. If η is a proportionality constant independent of the shear rate the fluid is said to be Newtonian. However, if the constituent molecules show preferred orientations, this will alter the retarding forces between adjacent fluid elements and hence the internal friction or viscosity coefficient. This non-Newtonian effect will occur in solutions containing highly asymmetric or easily deformable molecules and at high shear rates (Batchelor, 1967); this forms the basis of flow birefringence experiments (see 1.5.3). For characterizing the macromolecule in solution we can set the conditions (i.e. very low shear rates) so that the Newtonian condition prevails, whereas the chemical engineer would be more interested in the general flow properties.

Using equation (4) we can simply relate the viscosity coefficient to the energy dissipation during flow. Writing σ as a tangential force per unit area (F/A) and the shear rate as the velocity gradient ($(dx/dt)/\Delta y$):

$$\frac{F}{A} = \eta \frac{1}{\Delta y} \frac{dx}{dt}$$

Multiplying both sides by G:

$$\frac{F\ dx}{A\Delta y dt} = \eta\ G^2$$

Since $A\Delta y$ is the volume of the element under consideration, then

$$\left\langle \frac{dW}{dt} \right\rangle = G^2 \eta \qquad (5)$$

where $\langle dW/dt \rangle$ is the mean energy dissipated per unit volume.

The effect of dissolved or suspended macromolecules which are assumed to occupy a volume ϕ of fluid, is to disturb the streamlines of the fluid motion and to reduce the volume of the fluid in which the same overall deformation takes place. Thus the internal friction, the viscosity

coefficient and hence the energy dissipated is increased. This increase can be represented by:

$$\left\langle \frac{dW}{dt} \right\rangle_{inc} = G^2(\eta - \eta_o) = G^2 \eta_o \nu\phi \qquad (6)$$

where η is the viscosity coefficient of the solution and η_o that of the solvent. Rewriting:

$$\eta = \eta_o (1 + \nu\phi) \qquad (7)$$

Here ν is defined as the viscosity increment and is a function of the shape of the particle. Again, rewriting equation (7):

$$\frac{\eta}{\eta_o} - 1 = \eta_{sp} = \nu\phi$$

where η_{sp} is the specific viscosity. This equation only applies to an infinitely dilute solution in which no solute-solute interactions occur. For finite concentrations:

$$\eta_{sp} = \nu\phi + \nu_1\phi^2 + \nu_2\phi^3 + \ldots \ldots$$

or, replacing ϕ by $c\bar{v}_s$, where c is the concentration and $\bar{v}_s$ the swollen specific volume:

$$\eta_{red} = \frac{\eta_{sp}}{c} = \nu\bar{v}_s + \nu_1\bar{v}_s^2 c + \nu_2\bar{v}_s^3 c^2 + \ldots \ldots$$

where η_{red} is the reduced specific viscosity. As the concentration approaches zero, η_{red} tends to a limiting value, known as the intrinsic viscosity, $[\eta]$. This can therefore be found by extrapolating a plot of η_{red} versus concentration to infinite dilution, and, if the swollen specific volume, $\bar{v}_s$ is known (section 1.1.2.), ν can also be found:

$$\nu = \frac{[\eta]}{\bar{v}_s} = \frac{[\eta]M_r}{V_e N_A} \qquad (8)$$

An approximate value for ν can be estimated for 'globular' proteins by using the partial specific volume $\bar{v}$ and assuming that $\bar{v}_s / \bar{v}$ is ~ 1.4 for globular proteins. A full review of the experimental techniques for determining the intrinsic viscosity, $[\eta]$ is given by Yang (1961).

Einstein (1906, 1911) was the first to determine an explicit value for ν for a specific particle shape, i.e. a sphere, by solving the equations of motion for the flow using spherical harmonics. His assumptions were:

(i) the particles are large enough compared to the solvent molecules so that the surrounding fluid can be regarded as a continuum and Euler's (Batchelor, 1967) equations concerning the change of flow through specific volume elements rather than the complicated Lagrange equations for particle motion can be used,

(ii) the dimensions of the particles are however considered very much less than the spatial variations in the velocity flow field,

(iii) the flow rates are small enough so that squared terms concerning the velocity (and hence normal stress effects) can be neglected and that the inertia or mass forces can be neglected.

Using these assumptions and considering the increase in the average dissipation of energy per unit volume, he found that $\nu = 2.5$, and was independent of particle size. This result has been confirmed experimentally for polystyrene latex spheres by Cheng & Schachman (1955).

Jeffrey (1922) attempted to extend this theory to find ν as a function of axial ratio for ellipsoids of revolution, using ellipsoidal harmonics to solve the equations for the fluid flow. Owing to the non-isotropic nature of ellipsoids, the hydrodynamic torques on the ellipsoids were shown to have two effects:

(a) the first effect tends to make the particle rotate on average with the local undisturbed angular velocity of the fluid,

(b) the second effect tends to orient the minor axis parallel to the flow for prolate ellipsoids and perpindicular to the flow for oblate ellipsoids.

As a result, the fluid is no longer isotropic and an energy dissipation analysis fails to give a unique value for the axial ratio for a given value of ν (Brenner, 1972a). However, if the particles are sufficiently small the randomizing effect of the Brownian motion of the surrounding solvent molecules counteracts the orientational tendancy of the hydrodynamic torque (b) so that the particles are randomly oriented (Simha, 1940) and rotate on average with the local angular velocity of the fluid. The solution is then statistically isotropic, allowing an energy dissipation analysis to be used to obtain an unambiguous solution for ν in terms of the axial ratio for prolate and oblate ellipsoids of revolution. Simha (1940) was thus able to obtain a formula which has been shown to give good agreement with experiment (Mehl, Oncley & Simha, 1940):

$$\nu = \frac{1}{ab^2}\left\{\frac{2\alpha_o''}{15b^2\alpha_o'\beta_o'} + \frac{7}{15b^2\alpha_o'} + \frac{2}{5}\left[\frac{\beta_o'(a^2+b^2)+2\beta_o''}{\beta_o'[2a^2b^2\beta_o'+(a^2+b^2)\beta_o'']}\right]\right\} \tag{9}$$

where a,b,b are the three semi-axes of the ellipsoid ($b > a$ for oblate and $b < a$ for prolate), and the α_o' etc. which depend on a and b are elliptic integrals given by Jeffrey (1922) (Appendix I). This relation could be solved numerically for both cases and a table of values for ν as a function of axial ratio was given by Mehl, Oncley & Simha (1940).

The function is plotted in Figure 4. In the limit of large axial ratio p (=b/a)

$$\nu \sim \frac{1/p^2}{15(\ell n(2/p)-3/2)} + \frac{1/p^2}{5(\ell n(2/p)-1/2)} + \frac{14}{15} \qquad \text{(prolate)} \tag{10a}$$

$$\nu \sim \frac{16}{15} \tan^{-1}(p) \qquad \text{(oblate)} \tag{10b}$$

These formulae agree with the independent derivations of Kuhn & Kuhn (1945) and Kirkwood (1967).

Simha apparently did not assume that the particles were on average rotating with the local angular velocity of the fluid but with zero angular velocity. This objection was raised by Saito (1951) who however obtained exactly the same result (equation 9) despite assuming particles on average rotating with the same local angular velocity of the fluid. He suggested that Simha "probably made some error in his calculation" without actually finding it. We will show in the next Chapter that Simha had apparently arrived at the correct result by making the wrong assumption and then missing out a whole series of terms in his calculation.

1.4. The Translational Frictional Property of Macromolecular Solutes

The ease with which a macromolecule moves through its solution under the influence of an applied external force field will depend on its shape and size. The coefficient generally used to describe this ease is the frictional coefficient, f, defined as the ratio of the frictional force to the terminal velocity of the particle. Stokes (1851) using spherical harmonics again and assumptions similar to Einstein's (section 1.3) derived the well-known relation between the frictional coefficient f and

the radius R of a spherical particle:

$$f = 6\pi\eta_o R \tag{11}$$

where η_o is the viscosity of the solvent. Perrin (1936) and independently Herzog, Illig and Kudar (1934) extended Stokes equation to cover the case of general ellipsoidal particles:

$$\frac{f}{f_o} = \frac{2}{(abc)^{1/3}\int_0^{\infty} \frac{d\lambda}{[(a^2+\lambda)(b^2+\lambda)(c^2+\lambda)]^{\frac{1}{2}}}} \tag{12}$$

where f_o is the corresponding coefficient for a sphere of the same volume:

$$f_o = 6\pi\eta_o(abc)^{1/3} = 6\pi\eta_o\left(\frac{3V_e}{4\pi}\right)^{1/3} \tag{13}$$

V_e is the molecular swollen volume, defined in section 1.1.2. The integral in equation (12) is elliptic and could only be solved for the special case of ellipsoids of revolution. For prolate ellipsoids ($p = (b/a) < 1$):

$$\frac{f}{f_o} = \frac{(1 - p^2)}{p^{2/3}\tan^{-1}(p^2 - 1)^{\frac{1}{2}}} \tag{14a}$$

and for oblate ellipsoids ($p = (b/a) > 1$)

$$\frac{f}{f_o} = \frac{(p^2 - 1)}{p^{2/3}\tan^{-1}(p^2-1)^{\frac{1}{2}}} \tag{14b}$$

and can easily be plotted as a function of axial ratio (Figure 5). The translational frictional ratio f/f_o can be measured experimentally either from a translational diffusion experiment, where the driving force is a concentration gradient, or from ultracentrifugation, where the driving force is a centrifugal field.

1.4.1. Translational Diffusion

The translational diffusion coefficient, D, is related to the frictional coefficient, f, at a particular particle concentration, c, by the relation:

$$D_c = \frac{kT}{f}\left\{1 + c\,\frac{\partial \ell n \gamma}{\partial c}\right\} \qquad (15)$$

(van Holde, 1971), where γ is the 'activity coefficient', a measure of the concentration gradient. Extrapolating D_c to infinite dilution gives the Einstein relation (Einstein 1905, Tanford, 1961):

$$D = \frac{kT}{f} \qquad (16)$$

By assuming the concentration gradient to be in one direction only, and applying Fick's laws (Tanford, 1961) for a two-component system, a simple relation for finding D experimentally can be derived, in terms of the area under, A, and the maximum height of, H, a concentration gradient (dc/dx) versus distance (x) curve:

$$\left(\frac{A}{H}\right)^2 = 4\pi D_c t$$

Thus a plot of $(A/H)^2$ versus time, t, in a 'free diffusion of a sharp boundary experiment' will give D_c from the gradient (Tanford, 1961, van Holde, 1971). D_c can be extrapolated to infinite dilution after repeating the procedure for several solute concentrations. Unfortunately, few laboratories have the apparatus required for an accurate determination of D using this method. A fast and accurate method for determining diffusion coefficients has been developed using quasi-elastic laser light scattering (Chu, 1974, Cummins & Pike, 1973, Berne & Pecora, 1974); the fluctuations of solute particles from the equilibrium state are a function of the diffusion

coefficients and with adequate instrumentation for signal analysis can be time-resolved.

From equation (16), the frictional ratio can be found from the translational diffusion coefficient using the relation

$$\frac{f}{f_o} = \frac{D_o}{D} \qquad (17)$$

where D_o is the translational diffusion coefficient for a sphere of the same volume and molecular weight:

$$D_o = \frac{kT}{f_o} = \frac{kT}{6\pi\eta_o}\left(\frac{4\pi}{3V_e}\right)^{1/3} \qquad (18)$$

1.4.2. Sedimentation Velocity

In a sedimentation velocity experiment, using an analytical ultracentrifuge (van Holde, 1971), the macromolecules quickly attain the terminal velocity, whence

$$\frac{M_r}{N_A}(1 - \bar{v}\rho_o)\omega^2 r = f\frac{dr}{dt}$$

where ρ_o is the solution density, r the distance from the centre of rotation of the solution/solvent boundary, ω the speed of rotation and $M_r(1 - \bar{v}\rho_o)/N_A$ the 'buoyant mass' defined in section 1.1.1. Rearranging:

$$\frac{M_r(1 - \bar{v}\rho_o)}{N_A f} = \frac{dr/dt}{\omega^2 r} = s_c \qquad (19)$$

where s_c is the sedimentation coefficient at a particular solute concentration. In a sedimentation velocity experiment the movement of the boundary between solution and solvent is monitored as a function of time using the property of change of refractive index with change in

concentration, hence optical techniques such as scanning Schlieren optics or ultra-violet absorption can be used (Lloyd, 1974). If we rearrange and integrate equation (19) we find that

$$s_c = \frac{1}{\omega^2} \frac{\Delta \ell n r}{\Delta t}$$

thus by plotting $\log_e r$ versus t and knowing the angular velocity ω, s_c can be found from the gradient. The sedimentation coefficient s_c is a function of solute concentration, thus is normally extrapolated to infinite dilution to give the sedimentation coefficient, s, which is characteristic of any macromolecular solute. From equation (19) it can be seen that the frictional ratio f/f_o will be given by

$$\frac{f}{f_o} = \frac{s_o}{s}$$

where s_o is the sedimentation coefficient for a compact sphere of the same molecular weight and volume. From equations (19) and (13):

$$s_o = \frac{M_r(1 - \bar{v}\rho_o)}{N_A f_o} = \frac{M_r(1 - \bar{v}\rho_o)}{N_A 6\pi\eta_o} \cdot \left(\frac{4\pi}{3V_e}\right)^{1/3} \qquad (20a)$$

and thus the frictional ratio can be found, provided s, M_r, $\bar{v}$, ρ_o, η_o and the swollen molecular volume, V_e are known:

$$\frac{f}{f_o} = \frac{M_r(1 - \bar{v}\rho_o)}{N_A 6\pi\eta_o s} \left(\frac{4\pi}{3V_e}\right)^{1/3} \qquad (20b)$$

1.5. The Rotational Frictional Property of Macromolecular Solutes

The ability of a macromolecule to rotate under the influence of the local Brownian motion of the neighbouring solvent molecules will depend on its size and shape. By analogy with the translational frictional

coefficient, we can define, for rotation about a specific particle axis, a rotational frictional coefficient, ζ_i, as the torque which must be applied to cause the particle to rotate with unit angular velocity. For a general ellipsoidal particle there will be three rotational frictional coefficients corresponding to rotation about each of the three axes; for an ellipsoid of revolution there will be two, and for a spherical particle, one. Each rotational frictional coefficeint can be related to a rotational diffusion constant by analogy with the Einstein relation (1905) (equation 16):

$$\theta_i = \frac{kT}{\zeta_i} \qquad (21)$$

where θ_i is defined as the ratio of the mean squared angular displacement of the axis to the time elapsed (Tanford, 1961). In a typical rotational frictional experiment an initial orientation of the macromolecule is produced by some external field. If, for example, the macromolecules in a solution are oriented with their "a" axis parallel to an orienting field and the field is suddenly removed, the macromolecules will then relax due to the Brownian motion and tend to assume a random configuration by rotating about the b and c axes. We therefore conveniently define a rotational relaxation time in terms of the rotational diffusion constants (θ_b, θ_c about the b,c axes respectively) by

$$\varrho_a = \frac{1}{\theta_c + \theta_b} \qquad (22a)$$

There will be similar relations describing relaxation of the b and c axes:

$$\varrho_b = \frac{1}{\theta_c + \theta_a} \quad ; \quad \varrho_c = \frac{1}{\theta_a + \theta_b} \qquad (22b,c)$$

By analogy with the translational frictional case, Stokes (1880) using spherical harmonic solutions of the equations of motion with the boundary condition that the fluid in contact with the particle rotates with the same angular velocity (i.e. the 'no-slip' condition) derived an equation linking the rotational frictional coefficient with its radius, R:

$$\zeta = 8\pi\eta_o R^3 \qquad (23)$$

Edwardes (1893) extended this equation to the case of general ellipsoidal particles. After a correction for a numerical error (Perrin, 1934), these are:

$$\zeta_a = \frac{16\pi\eta_o}{3} \quad \frac{b^2 + c^2}{b^2\beta_o + c^2\gamma_o}$$

$$\zeta_b = \frac{16\pi\eta_o}{3} \quad \frac{c^2 + a^2}{c^2\gamma_o + a^2\alpha_o}$$

$$\zeta_c = \frac{16\pi\eta_o}{3} \quad \frac{a^2 + b^2}{c^2\gamma_o + a^2\alpha_o} \qquad (24)$$

where again the α_o etc. are elliptic integrals defined by Jeffrey (1922) - see Appendix I. The expressions on the right hand side of equations (24) are functions not only of shape but of volume as well; the corresponding rotational frictional ratios however, are not.

$$\frac{\zeta_a}{\zeta_o} = \frac{\theta_o}{\theta_a} = \frac{2}{3abc}\ \frac{b^2 + c^2}{b^2\beta_o + c^2\gamma_o}$$

$$\frac{\zeta_b}{\zeta_o} = \frac{\theta_o}{\theta_b} = \frac{2}{3abc}\ \frac{c^2 + a^2}{c^2\gamma_o + a^2\alpha_o}$$

$$\frac{\zeta_c}{\zeta_o} = \frac{\theta_o}{\theta_c} = \frac{2}{3abc}\ \frac{a^2 + b^2}{a^2\alpha_o + b^2\beta_o} \qquad (25)$$

where ζ_o $(=8\pi\eta_o abc)$ & θ_o $(=kT/\zeta_o)$ are the corresponding coefficients for spheres of the same volume, and can be found experimentally only if the swollen molecular volume, V_e is known:

$$\zeta_o = 6\eta_o V_e\ ,\ \theta_o = kT/6\eta_o V_e \qquad (26a,b)$$

The corresponding rotational relaxation time ratios are:

$$\frac{\varrho_a}{\varrho_o} = \frac{2}{\left[\frac{\theta_b}{\theta_o} + \frac{\theta_c}{\theta_o}\right]}$$

$$\frac{\varrho_b}{\varrho_o} = \frac{2}{\left[\frac{\theta_c}{\theta_o} + \frac{\theta_a}{\theta_o}\right]}$$

$$\frac{\varrho_c}{\varrho_o} = \frac{2}{\left[\frac{\theta_a}{\theta_o} + \frac{\theta_b}{\theta_o}\right]} \qquad (27a)$$

where $\varrho_o = 1/2\,\theta_o$. (27b)

Unfortunately, as for the translational frictional coefficients, the elliptic integrals could only be solved analytically for the special case of ellipsoids of revolution of semi-axes a, b=c (Gans, 1928, Perrin, 1934). Although numerically equivalent, Gans uses the less manageable 'eccentricity' ($\epsilon = 1 - b/a$) rather than the axial ratio ($p = b/a$), hence the equations of Perrin are generally used:

$$\frac{\zeta_a}{\zeta_o} = \frac{\theta_o}{\theta_a} = \frac{2}{3}\frac{(1 - p^2)}{(1 - p^2 S)}$$

$$\frac{\zeta_b}{\zeta_o} = \frac{\theta_o}{\theta_b} = \frac{2}{3}\frac{(1 - p^4)}{p^2[S(2-p^2) - 1]} \qquad (28a)$$

where

$$S = (1 - p^2)^{-\frac{1}{2}} \ell n\{[1 + (1-p^2)^{\frac{1}{2}}]/p\}$$

for a prolate ellipsoid ($p<1$), and

$$S = (p^2 - 1)^{-\frac{1}{2}} \tan^{-1}[(p^2 - 1)^{\frac{1}{2}}]$$

for an oblate ellipsoid ($p>1$).

The rotational diffusion ratio θ_i/θ_o (i=a,b) can be related to experimental parameters using equations (26b):

$$\frac{\theta_i}{\theta_o} = \frac{\overline{6\eta_o V_e}}{kT}\,\overline{\theta_i} \qquad (28b)$$

The corresponding rotational relaxation time ratios were also given by Perrin (1934) but contained an error of sign involving S. The correct result was given by Koenig (1975):

$$\frac{\varrho_a}{\varrho_o} = \frac{\theta_o}{\theta_b} = \frac{2(1 - p^4)}{3p^2[S(2-p^2) - 1]}$$

$$\frac{\varrho_b}{\varrho_o} = \frac{2}{\left(\frac{\theta_a}{\theta_o} + \frac{\theta_b}{\theta_o}\right)} = \frac{4(1 - p^4)}{3[p^2S(1-2p^2) + 1]} \qquad (29a)$$

These may be related to experimental parameters by combining equations (26b, 27b):

$$\frac{\varrho_i}{\varrho_o} = \sqrt{\frac{kT}{3\eta_o V_e}}\ \varrho_i \qquad (29b)$$

All these functions ($\zeta_i/\zeta_o = \theta_o/\theta_o$, ϱ_i/ϱ_o) are plotted as functions of axial ratio in Figure 6. It should also be pointed out that, like the translational functions the rotational diffusion coefficients and relaxation times are functions of concentration (Riddiford & Jennings, 1967) and should be extrapolated to infinite dilution. The same is also true for the harmonic mean relaxation time, the birefringence decay constants and the fluorescence depolarisation relaxation times mentioned below. The various experimental methods for determining all these shape parameters will now be discussed.

1.5.1. Dielectric Dispersion

The capacity of a condenser filled with a solution of the macromolecule is measured as a function of the applied sinusoidal voltage across it

(Edsall, 1953). The 'dielectric increment' or increase in the dielectric constant, ε, due to the presence of the solute is given by

$$\Delta\varepsilon = \varepsilon - \varepsilon_o = \frac{C}{C_v} - \frac{C_o}{C_v} \qquad (30)$$

where ε_o is the dielectric constant of the solvent and C, C_o and C_v are the capacities of respectively, the solution, solvent and vacuo. At sufficiently small frequencies, the dipolar macromolecules can keep pace with the alternating field, and the dielectric constant will remain at its 'static' value. At sufficiently high fields, the rotation of the macromolecule about a particular axis will no longer follow the field and its contribution, $\Delta\varepsilon_\infty$ to the dielectric constant is that of a non-polar substance (Oncley, 1940); thus over a certain critical range characteristic of the size and shape of the macromolecule, the dielectric constant decreases as the frequency increases. The frequency corresponding to the mid-point of the dispersion curve is known as the 'critical frequency'. For a general particle with three rotational relaxation times ϱ_a, ϱ_b, ϱ_c, there will be three critical frequencies:

$$\nu_a = 2\pi\varrho_a \quad ; \quad \nu_b = 2\pi\varrho_b \quad ; \quad \nu_c = 2\pi\varrho_c \qquad (31)$$

For an ellipsoid of revolution there will be two (since $\varrho_b = \varrho_c$) or one, either if the dipolar axis is parallel to the rotation axis of symmetry or for a spherical particle. Typical dielectric dispersion curves for ellipsoids of revolution of various axial ratios are shown in Figure 7 (from Oncley, 1940)

Even in the most favourable case, $\theta = 45^o$, resolution is poor for axial ratios less than 9 (Squire, 1978). Application of this method is

also limited by the fact that, due to electrode polarization, only solutions of low ionic strength can be used, thus restricting the use to proteins of high solubility.

1.5.2. Electric Birefringence

Polarized light incident on a solution of macromolecules oriented by an elctric field will be split into perpendicular components because the refractive index will be different for directions parallel and perpendicular to the electric dipole moment (Benoit, 1951). The solution is then said to be birefringent and the amount of birefringence will depend on the nature and concentration of the macromolecules.

The decay due to Brownian motion of the birefringence when the field is suddenly switched off is most interesting since this will be independent of the electric properties of the macromolecules (apart from the initial amplitude of the decay) but dependent on their size and asymmetry, assuming the solution to be homogeneous. The solution must be rendered homogeneous by, say, ultracentrifugation for removing larger impurities, followed by gel filtration for fine purification. The number of terms in the exponential decay will be dependent on the particle asymmetry, assuming that the particles are small enough so that the Rayleigh - Gans - Debye scattering theory applies (i.e. particle dimensions less than $\lambda/20$). Ridgeway (1966, 1968) has shown that a general particle will have two relaxation times, τ_+, τ_- or two decay constants, θ_+ $(=1/6\tau_+)$, θ_- $(=1/6\tau_-)$:

$$\Delta n = \frac{N}{2n_\ell} \left(A_+ e^{-6\theta_+ t} + A_- e^{-6\theta_- t}\right) \qquad (32)$$

where Δn is the birefringence, N is the number density of particles in

suspension, n_ℓ the refractive index of the solvent and $A_{\pm}$ complicated expressions depending on the initial particle orientations and their dielectric and diffusion properties. Unfortunately, although Ridgeway provided relationships linking $\theta_{\pm}$ with the size and shape of general tri-axial ellipsoids (see Chapters 3 and 4), only one relaxation time has been resolved from the experimental exponential decays for homogeneous solutions. Thus the method has been restricted to ellipsoids of revolution ($A_- = 0$) for which Benoit (1951) had shown previously that, for an initial birefringence n_o,

$$\Delta n = \frac{N}{2n_\ell} A e^{-6\theta_b t} = n_o e^{-6\theta_b t} \qquad (33)$$

assuming the electric dipole axis coincides with the rotational axis of symmetry. For spherical particles there would be no birefringence.

1.5.3. Flow Birefringence

The aligning field can also be produced, if the macromolecules are highly asymmetric, by large flow velocity gradients in the annular space between two concentric cylinders, one rotary and one stationary (van Holde, 1971, Squire, 1978). The orientation of the macromolecules will again be opposed by rotational Brownian motion, and for a constant shear rate, there will be an equilibrium distribution of orientation states. Results for early studies are discussed by Cerf and Scheraga (1952) and by Tanford (1961). This method has the advantage that the steady state birefringence can now be used to derive shape parameters, since this will be independent of the electric properties of the macromolecule. However, the method has the serious disadvantage in that relaxation experiments are virtually impossible,

and also the use is restricted to highly asymmetric molecules (Squire, 1978).

1.5.4. Fluorescence Depolarization

This method applies to those macromolecules that possess a fluorescent group or a chromophore (Cantor & Tao, 1971). If an electron in a chromophore is excited to a higher energy state by the absorption of radiation, then instead of the energy being dissipated non-radiatively in the form of heat as it returns to the ground state, it loses only part of its energy as heat as it returns to the lowest vibrational level of the excited state, but then re-radiates the rest. This will necessarily be of lower energy (hence longer wavelength) than the incident radiation. This phenomenon is called fluorescence.

If the macromolecule is irradiated with polarized light, and if, in the 10^{-8} to 10^{-7} seconds it takes for the energy to be re-radiated the macromolecule has changed its orientation due to Brownian motion, there will be a net depolarization of the incident light. If the solution is continuously irradiated then a steady state depolarization will be reached depending on the ratio of the fluorescence decay time, τ^* to the harmonic mean of the three rotational relaxation times (equations 27), τ_h (Perrin, 1934):

$$\left(\frac{1}{P} - \frac{1}{3}\right) = \left(\frac{1}{P_o} - \frac{1}{3}\right) \left(1 + \frac{3\tau^*}{\tau_h}\right) \qquad (34)$$

P is the polarization (i.e. the ratio of the difference in intensities of light polarized parallel and perpindicular to the incident beam to their sum), P_o is the intrinsic polarization of the fluorescence (the polarization that would be observed if no rotation had occurred) and τ_h is defined by

$$\frac{1}{\tau_h} = \frac{1}{3}\left(\frac{1}{\varrho_a} + \frac{1}{\varrho_b} + \frac{1}{\varrho_c}\right) \qquad (35)$$

for general ellipsoids, or for ellipsoids of revolution ($\varrho_b = \varrho_c$):

$$\frac{1}{\tau_h} = \frac{1}{3}\left(\frac{1}{\varrho_a} + \frac{2}{\varrho_b}\right)$$

The harmonic mean relaxation time ratio τ_h / τ_o can thus be plotted as a function of axial ratio (Figure 8), where τ_o is the corresponding coefficient for a sphere of the same molecular weight and volume:

$$\tau_o = \frac{3\eta_o V_e}{kT} \qquad (36a)$$

Thus τ_h / τ_o can be related to experimental parameters by:

$$\frac{\tau_h}{\tau_o} = \frac{kT\tau_h}{3\eta_o V_e} \qquad (36b)$$

Equation (34) is not particularly useful as it stands, since neither P_o nor τ_h are known. If τ_h is approximated by $\tau_h \sim \tau_o$ (i.e. $= 3\eta_o V_e/kT$) then:

$$\left(\frac{1}{P} - \frac{1}{3}\right) = \left(\frac{1}{P_o} - \frac{1}{3}\right)\left(1 + \frac{kT\tau^*}{\eta_o V_e}\right) \qquad (37)$$

If measurements are then made in solutions of varying viscosity (for example by adding glycerol) and/or temperature, (1/P -1/3) can be plotted against T/η_o, $1/P_o$ can be found from the intercept and hence τ_h

from the gradient, assuming τ^* can be found independently. A major disadvantage of this method is that by adding glycerol or changing the temperature the swelling due to solvation may be altered: also an independent estimate for τ^* is required.

A more accurate method in principle is nanosecond fluorescence depolarization decay (Cantor & Tao, 1971). Here the solution is irradiated with polarized light pulses of very short duration (~1ns). The anisotropy, A is measured by determining the intensity of emission polarized parallel to ($I_{\parallel}$) and perpindicular to ($I_{\perp}$) the incident pulse:

$$A = \frac{I_{\parallel} - I_{\perp}}{I_{\parallel} + 2I_{\perp}} \qquad (38)$$

For a rigid spherical macromolecule, the anisotropy decay is described by a single exponential term (Jablonski, 1961)

$$A(t) = A_o e^{-t/\tau_o} \qquad (39)$$

with $\tau_o = \eta_o V_e/kT$. For a rigid ellipsoid of revolution, Memming (1961) and Wahl (1966) have shown that the anisotropy is a sum of three exponential terms:

$$A(t) = \alpha_1 e^{-t/\tau_1} + \alpha_2 e^{-t/\tau_2} + \alpha_3 e^{-t/\tau_3} \qquad (40)$$

where

$$\tau_1 = \frac{1}{6\theta_b} \quad ; \quad \tau_2 = \frac{1}{5\theta_b + \theta_a} \quad ; \quad \tau_3 = \frac{1}{2\theta_b + 4\theta_a} \qquad (41)$$

The fluorescence decay time ratios are plotted in Figure 9 where τ_o is the corresponding coefficient for a sphere of the same molecular weight and volume:

$$\tau_o = \frac{\eta_o V_e}{kT} = \frac{4\pi\eta_o ab^2}{3kT}$$

Thus the fluorescence anisotropy decay time ratios can be related to experimental parameters by

$$\frac{\tau_j}{\tau_o} = \frac{kT\tau_j}{\eta_o V_e} \qquad (j=1,2,3) \tag{42}$$

The values of the component amplitudes α_1, α_2, α_3 and hence the dominant relaxation time will depend on the angle between the transition moment of the chromophore to the rotation axis of symmetry of the ellipsoid of revolution. Unfortunately, resolution of a multi-term exponential decay into its components is notoriously difficult (Jost, 1978), even for relaxation times differing in orders of magnitude; this is coupled to the problem that the observed decay will be a convolution of the finite cut-off time of the incident pulse, the fluorescence decay and the anisotropy decay. There are also more serious problems:

(i) since the fluorescence itself decays within about 10ns, only molecules with very short relaxation times can be investigated,

(ii) most macromolecules do not contain a chromophoric group such as tryptophan; thus one must be introduced. This may significantly alter the true conformation of the molecule,

(iii) even if the macromolecule contains tryptophan, the decay is not perfectly exponential, due to interference between the side chain and the indole ring,

(iv) rotation of the chromophore, or of a fragment of the macromolecule to which the chromophore is attached, with respect to the rest of the macromolecule may occur: Munro et al (1979) have given evidence for internal rotation of the tryptophan residue in Staphylococcus aureus nuclease B (M_r = 14,100) and Pseudomonas aeruginosa azurin (M_r = 14,000).

1.6. Scattering

Absorption and hence fluorescence phenomena can only occur when the frequency of the exciting radiation is the same as or near to that of an allowed transition frequency of the molecule. However, at other wavelengths electro-optic interaction can still occur; the electric vector of the incident radiation polarizes the molecule by attracting the nuclear mass and repelling the electron clouds. The frequency of oscillation of the incident radiation is the same as that of the induced oscillating dipole; however, the waves emitted are by Huyghens principle spherical and hence the radiation is scattered in all directions.

The scattering by a solution of macromolecules is most rigorously analysed by considering the local concentration fluctuations of the solution; however, if we consider the particle as small compared with the wavelength of the incident light and the solution to be so dilute so that each particle can be considered independently, relations can be derived between particle shape in terms of the 'radius of gyration' (Tanford, 1961) and the scattering (van de Hulst, 1957). For small particles ($<\lambda/20$) interference effects between radiation scattered by different parts of the

macromolecule can be neglected, and the following relation between molecular weight, M_r and the scattering can be derived:

$$\frac{Hc}{\tau} = \frac{1}{M_r} + 2B.c$$

where c is the particle concentration, H is the scattering constant ($\alpha \lambda^{-4}$, and the square of the refractive index increment, dn/dc), B the second virial coefficient and τ is a measure of the relative scattering perpindicular to the incident beam (i.e. the fraction of light scattered (van Holde, 1971)). Hence if Hc/τ is plotted versus concentration, the molecular weight can in principle be determined from the intercept. For large particles ($d \sim \lambda/20$) destructive interference occurs between light scattered from different parts of the macromolecule. Light scattered in the forward direction cannot however be subject to destructive interference. Unfortunately this cannot be viewed directly, but if the scattering is studied over a range of angles it can be extrapolated to the forward direction. This involves extrapolating to zero-angle and to zero-concentration using the so-called Zimm plot (Zimm, 1948, Stacey, 1956, Tanford, 1961). The slope of the c=0 line gives the radius of gyration of the particle, R_G, i.e. the mean extension of mass from the centre of gravity. For a sphere of radius R, $R_G = \sqrt{3/5}\, R$, and for a large rod of length L, $R_G = L/\sqrt{12}$, thus light scattering can be used to obtain information about conformation in solution, where particular models for which R can be specified are applicable. Holtzer and Lowey (1956) showed by this method that L = 1500 $\mathring{A}$ if myosin could be reasonably modelled by a long rod. Martin (1964) has shown that the radius of gyration can be related to the axial ratio of the equivalent ellipsoid of revolution provided that the swollen volume is known:

$$R_G^2 = \left(\frac{3V_e}{4\pi}\right)^{2/3} \left(\frac{5p^{4/3} + 4p^{-2/3}}{15}\right) \tag{43a}$$

for a prolate ellipsoid and

$$R_G^2 = \left(\frac{3V_e}{4\pi}\right)^{2/3} \left(\frac{p^{4/3} + 2p^{-2/3}}{5}\right) \tag{43b}$$

for an oblate ellipsoid.

An explicit relation relating R_G to axial ratio alone can be found by 'reducing' it

$$(R_G)_{red} = \left(\frac{4\pi}{3V_e}\right)^{1/3} R_G = \left(\frac{5p^{4/3} + 4p^{-2/3}}{15}\right)^{\frac{1}{2}} \tag{44a}$$

for a prolate ellipsoid and

$$(R_G)_{red} = \left(\frac{4\pi}{3V_e}\right)^{1/3} R_G = \left(\frac{p^{4/3} + 2p^{-2/3}}{5}\right)^{\frac{1}{2}} \tag{44b}$$

for an oblate ellipsoid.

This is plotted in Figure 10. Experimental determination of $(R_G)_{red}$ requires of course a knowledge of V_e.

The same analysis can be used for laser light scattering as this gives good time resolution for rapidly changing solutions (for example aggregation of macromolecules, randomly coiled macromolecules). However a major difficulty with all light scattering experiments is that all

solutions, glassware etc., must be dust free; removal, without damage to the biological solute, poses great difficulties. Due to diffraction effects it is also difficult to measure scattering angles less than about five degrees, thus a clear extrapolation to zero angle may not be possible. Another major difficulty is that, since the resolving power depends on $(R_G/\lambda)^2$, the method fails for macromolecules below about 100 Å (although M_r may still be found). Reducing the wavelength of the incident radiation does not help (until down to the x-ray region) since below 200nm most biological materials absorb very strongly. A method of low angle x-ray scattering (LAXR) has also been developed (Beeman et al, 1957). However, due to very strong diffraction and interference effects, the scattering is almost entirely confined to a very narrow wavelength range. On the other hand, it is possible to collimate the x-ray beam much better than a light beam, thus measurements can be made to a low enough angle to a more reasonable extrapolation to zero angle.

Deductions about the size and shape of macromolecules from scattering information is generally restricted however, since any simple interpretation of the radius of gyration must assume that the macromolecule is homogeneous (uniform electron density). If, therefore, the particle contains fluid filled cavities or indentations or a monolayer of bound solvent, the dimensions of any assumed model calculated from the R_G will be incorrect. This problem does not apply to the determination of the hydrodynamic shape parameters considered previously since these phenomena do not depend on interactions with or properties of the interior of the macromolecules.

1.7. The Problem of Swelling due to Solvation

In order to determine from experimental data the ellipsoid

of revolution shape functions mentioned so far, a knowledge of the swelling due to solvation (i.e. V_e) is required:

$$\nu = \frac{[\eta]}{\bar{v}_s} \equiv \frac{[\eta]M_r}{N_A V_e} \tag{8}$$

$$\frac{f}{f_o} \equiv \frac{M_r(1 - \bar{v}\rho_o)}{N_A 6\pi\eta_o s} \left(\frac{4\pi}{3V_e}\right)^{1/3} \tag{20b}$$

$$\frac{\theta_i}{\theta_o} = \frac{\zeta_o}{\zeta_i} = \frac{6\eta_o V_e}{kT}\theta_i \tag{28b}$$

$$\frac{\varrho_i}{\varrho_o} = \frac{kT}{3\eta_o V_e}\varrho_i \qquad (i = a,b). \tag{29b}$$

$$\frac{\tau_h}{\tau_o} = \frac{kT}{3\eta_o V_e}\tau_h \tag{36b}$$

$$\frac{\tau_j}{\tau_o} = \frac{kT}{\eta_o V_e}\tau_j \qquad (j=1,2,3) \tag{42b}$$

$$(R_G)_{red} = \left(\frac{4\pi}{3V_e}\right)^{1/3} R_G \tag{44}$$

The first significant attempt at dealing with this problem was due to Oncley (1941) using a graphical analysis: If V_e is fixed then a single value of the shape parameter being considered will correspond to a single value of the axial ratio. If, however, V_e is assumed to have a range of possible values, then a single value of the shape parameter will have a

'line solution' of possible values of the axial ratio. This is shown in Figures 11a and 11b for the viscosity increment and translational frictional coefficient. However, if line solutions for two or more of the different shape parameters are compared, then in principle a unique value for the axial ratio and effective volume can be found from the intersection. On the other hand, in practice these curves could only be made to intersect by imposing large experimental errors on the data, and in one case - pepsin - the curves do not cross at all (Figure 12). Here Oncley uses as his abscissa the 'hydration factor' w, related to the effective volume, V_e by:

$$w = \rho_o(\bar{v}_s - \bar{v}) = \rho_o \left[\frac{N_A V_e}{M_r} - \bar{v}\right]$$

A different approach would be to eliminate V_e simultaneously by combining any two of the shape parameters together. The effective volume can then also be found by back substitution into the equations. This naturally assumes, as does the Oncley approach, that the axial ratio and the swelling are the same for both types of experiment. Scheraga and Mandelkern (1953) combined equations (8) and (20b) to produce a swelling-independent function β (Figure 13):

$$\beta = \frac{N_A^{1/3}}{(16200\pi^2)^{1/3}} \quad \frac{\nu^{1/3}}{f/f_o} \qquad (45a)$$

or in terms of experimental parameters, from

$$\beta \equiv \frac{N_A \, s[\eta]^{1/3} \eta_o}{M_r^{2/3}(1 - \bar{v}\rho_o)100^{1/3}} \qquad (45b)$$

where $[\eta]$ is in ml/gm. Scheraga and Mandelkern also combined equation (8) with equations (28b) to produce swelling independent δ_a and δ_b functions (Figure 14), although in their original paper, only δ_b is given:

$$\delta_i = \frac{\zeta_o}{\zeta_i}\nu = \frac{\theta_i}{\theta_o}\nu \equiv \frac{6\eta_o\theta_i[\eta]M_r}{N_A kT} \tag{46}$$

(i=a,b)

Scheraga (1961) later combined (20b) with (28b) to produce swelling independent μ_a, μ_b functions (Figure 15) although again only μ_b was given:

$$\mu_i = \left(\frac{f_o}{f}\right)\left(\frac{\zeta_i}{\zeta_o}\right)^{1/3} \equiv \frac{3\pi^{2/3}s}{\theta_i^{1/3}} \cdot \frac{N_A(kT)^{1/3}\eta_o^{2/3}}{M_r(1-\bar{v}\rho_o)} = \frac{3\pi^{2/3}D}{\theta_i^{1/3}}\left(\frac{\eta_o}{kT}\right)^{2/3} \tag{47}$$

(i=a,b)

Squire <u>et al</u> (1968) combined equation (20b) with (29b) to produce swelling independent γ_a and γ_b functions:

$$\gamma_i = \left(\frac{f}{f_o}\right)^3 \frac{\rho_o}{\rho_i} \equiv \frac{1}{54\pi^2 N_A^3 kT} \cdot \frac{M_r^3(1-\bar{v}\rho_o)}{s^3\eta_o^2\rho_i} \tag{48}$$

(i=a,b)

Squire later (1970) combined (20b) with (36b) to give a swelling independent Ψ function (Figure 16)

$$\Psi\left(\frac{\tau_o}{\tau_h}\right)^{1/3}\left(\frac{f}{f_o}\right) \equiv \left(\frac{4\pi\eta_o}{kT}\right)^{1/3} \cdot \frac{M_r(1-\bar{v}\rho_o)}{6\pi\eta_o N_A s}\left(\frac{1}{\tau_h}\right)^{1/3} \tag{49}$$

Plots of the Squire γ_a and γ_b parameters as functions of axial ratio are given in Figure 16. A similar swelling independent function can be obtained by combining the viscosity increment, equation (8) instead of equation (20b) with (36b) (see Appendix II and Harding, 1980a):

$$\Lambda = \left(\frac{\tau_o}{\tau_h}\right) \nu \equiv \frac{3\eta_o[\eta]M_r}{N_A\, kT\, \tau_h} \tag{50}$$

(Figure 17). Also, by combining equation (8) instead of (20b) with equation (29b), swelling independent ε_a, ε_b functions are produced (Figure 18):

$$\varepsilon_i = \nu \frac{\varrho_o}{\varrho_i} \equiv \frac{3\eta_o[\eta]M_r}{N_A\, kT\, \varrho_i} \tag{51}$$

(i=a, b)

By combining (8) with the fluorescence anisotropy relaxation times (42b) three new functions, κ_1, κ_2, κ_3 are produced (Figure 19):

$$\kappa_j = \nu \frac{\tau_o}{\tau_j} = \frac{\eta_o[\eta]M_r}{N_A\, kT\, \tau_j} \qquad (j=1,2,3) \tag{52}$$

Alternatively, combining equation (20b) with equation (42b)(Figure 20):

$$\xi_j = \left(\frac{f}{f_o}\right)^3 \frac{\tau_o}{\tau_j} \equiv \frac{M_r^3 (1-\bar{v}\rho_o)^3}{162 N_A^3 kT \pi^2 \eta_o^2 s^3 \bar{\tau}_j} \qquad (j = 1,2,3) \tag{53}$$

As far as the author is aware, the Λ, ε_i, κ_j and ξ_j functions are new and have not been published before. These functions are tabulated for axial ratios between 1 and 10 (Table 1).

Martin (1964) eliminated the requirement of knowledge of the swollen volume for scattering experiments by combining (44) simultaneously with

either the translational frictional function (Figure 21):

$$\gamma \equiv \frac{R_G \eta_o D}{kT} \equiv \frac{R_G \eta_o N_A s}{M_r(1 - \bar{v}\rho_o)} = \frac{1}{6\pi} \frac{f_o}{f} \left(\frac{5p^{4/3} + 4p^{-2/3}}{15} \right)^{\frac{1}{2}}$$

(prolate ellipsoid)

$$= \frac{1}{6\pi} \frac{f_o}{f} \left(\frac{p^{4/3} + 2p^{-2/3}}{5} \right)^{\frac{1}{2}}$$

(oblate ellipsoid)

or the viscosity increment (Figure 22):

$$\alpha \equiv \frac{R_G}{[\eta]^{1/3} M_r^{1/3}} = \frac{75}{\pi N_A} \left(\frac{5p^{4/3} + 4p^{-2/3}}{15} \right)^{\frac{1}{2}} \cdot \frac{1}{\nu^{1/3}}$$

(prolate ellipsoid)

$$= \frac{75}{\pi N_A} \left(\frac{p^{4/3} + 2p^{-2/3}}{5} \right)^{\frac{1}{2}} \cdot \frac{1}{\nu^{1/3}}$$

(oblate ellipsoid)

where p is the axial ratio defined in section 1.4.

The molecular covolume has also been given as a function of shape and swollen volume by Nichol et al (1977) for prolate and oblate ellipsoids

$$U = N_A V_e \left\{ 2 + \frac{3}{2} \left(\frac{1 + \sin^{-1}\varepsilon}{\varepsilon(1 - \varepsilon^2)^{\frac{1}{2}}} \right) \right.$$

$$\left. \left(1 + \frac{1 - \varepsilon^2}{2\varepsilon} \ln \frac{1 + \varepsilon}{1 - \varepsilon} \right) \right\}$$

(54)

where the ellipticity ε is related to the axial ratio by

$$\varepsilon = \sqrt{1 - \frac{b^2}{a^2}}$$

for prolate ellipsoids (b<a), and

$$\varepsilon = \sqrt{1 - \frac{a^2}{b^2}}$$

for oblate ellipsoids (b>a). By 'reducing' U we obtain a function U_{red} in terms of shape alone:

$$U_{red} = \frac{U}{N_A V_e} = 2 + \frac{3}{2}\left(1 + \frac{1 + \sin^{-1}\varepsilon}{\varepsilon(1 - \varepsilon^2)^{\frac{1}{2}}}\right)\left(1 + \frac{1 - \varepsilon^2}{2\varepsilon} \ln \frac{1 + \varepsilon}{1 - \varepsilon}\right) \quad (55)$$

The covolume U can be found from a sedimentation equilibrium experiment in terms of the activity coefficient, as outlined by Nichol et al (1977) although in order to determine U_{red}, a knowledge of V_e is still required. Nichol et al (1977) however eliminated V_e by solving equation (55) simultaneously with the translational frictional ratio (equation 20b) to produce the swelling independent ψ function (not to be confused with the Squire Ψ function)

$$\psi = \frac{U_{red}}{162\pi^2}\left(\frac{f_o}{f}\right)^3 \equiv \frac{U \eta^3 N_A^2 s^3}{M_r^3 (1 - \bar{v}\rho_o)^3} \quad (56)$$

As seen from Figure 23, ψ has the advantage that no prior decision has to be made as to whether the macromolecule is better modelled either by a prolate or oblate ellipsoid. Unfortunately, for typical globular macromolecules (small axial ratios), the parameter is still very

sensitive to experimental error: this is clear from Nichol et al's results for ovalbumin, whose axial ratio they found to be 2.5:1 with a standard error of 3. This is largely due to the large number of terms on the right hand side of equation (56), several of them cubed.

U_{red} can of course be combined with any of the equations (8), (20b), (28b), (29b), (36b), (42b) to eliminate V_e. For example, if (55) is combined with the viscosity increment (8), a new swelling independent function is produced (Figure 24) (Harding, 1980b):

$$\Pi = \frac{U_{red}}{\nu} \equiv \frac{U}{[\eta]M_r} \qquad (57)$$

Values of the Π function for various axial ratios are given in Table 1. The results for hemoglobin are in excellent agreement with those found from x-ray crystallography (see Appendix III).

1.7.1. Hydrodynamic non-ideality: the R function

The viscosity, translational frictional and rotational parameters considered so far are normally those extrapolated to zero concentration in order to negate the effect of the net volume excluded by the particles and solute-solute interaction. However, the nature of the concentration dependence of these parameters, particularly the sedimentation coefficient "s" and the reduced specific viscosity, η_{sp}/c, has now been shown by Rowe (1977) to give valuable information as to the conformation and swelling in solution and also an estimate of the "goodness of fit" of an ellipsoid for the macromolecule in solution.

The variation of s and η_{sp}/c with concentration can be represented

by regression parameters k_s, and k_η:

$$s_c = s(1 - k_s c) \tag{58}$$

$$\frac{\eta_{sp}}{c} = [\eta]\ (1 + k_\eta c)\ . \tag{59}$$

where k_s and k_η are, respectively, the sedimentation and viscosity concentration regression coefficients. These approximate linear equations are valid only for dilute solutions. A universal equation has been derived by Rowe (see Appendix IV) for all solute concentrations up to ϕ_p, the critical packing fraction:

$$\frac{s_c}{s} \simeq \frac{f_o}{f} = \frac{[\eta]}{\eta_{sp}/c} = 1 - gc \tag{60a}$$

where

$$gc = \frac{kc - (2\phi_p - 1)(c\bar{v}_s/\phi_p)^2}{kc - 2\bar{v}_s c + 1} \tag{60b}$$

where $k=k_s$ (sedimentation) or $k=k_\eta$ (viscosity). This provides a more accurate method for extrapolating to infinite dilution to obtain $[\eta]$ and "s", and also for finding k_s and k_η, from a given set of data, by minimising:

$$\{w_i[s_i - f(k_s, \bar{v}_s, s, c_i, \phi_p)\ ]\}^2$$

(w_i = weight) (61)

This procedure is unstable if k_s, $\bar{v}_s$ and s (or the corresponding viscosity parameters) are all taken to be independent variables. However, if we assume $\bar{v}_s = k_s/4$ for globular proteins, or assume $\bar{v}_s$ from the ratio $\bar{v}_s/\bar{v}$

$= k'_\eta / k'_s$, where k'_η and k'_s are the parameters found from the approximate fit (equations 58 & 59), a stable fit may be found.

Rowe (1977) has shown that the swelling, $\bar{v}_s / \bar{v}$, can be found from:

$$\frac{\bar{v}_s}{v} = \frac{k_\eta}{k_s} \tag{62}$$

Therefore

$$V_e = \frac{M_r \bar{v}_s}{N_A} = \frac{M_r}{N_A} \cdot \frac{k_\eta}{k_s} \cdot \bar{v} \tag{63}$$

The value of $\bar{v}_s / \bar{v}$ and hence V_e thus found is independent of any assumed model for the protein. Since the determination of V_e by back substitution into the equations given at the beginning of 1.7. after the axial ratio has been determined is dependent on the model chosen (i.e. an ellipsoid of revolution), an estimate for the "goodness of fit" of an ellipsoid of revolution is now available by comparing the model dependent V_e with model independent V_e (or, equivalently, $\bar{v}_s$ or $\bar{v}_s / \bar{v}$).

This theory also provides a new shape function "R", which is independent of particle swelling:

$$R = \frac{2}{\nu} \left(1 + \left(\frac{f}{f_o} \right)^3 \right) \equiv \frac{k_s}{[\eta]} \tag{64}$$

Wales & Van Holde (1954) had previously reported that the ratio $k_s / [\eta]$ was some unknown function of shape and equal to 1.6 for spherical particles; this agrees with that predicted by equation (44) (Figure 13). R varies rather rapidly with axial ratio for ellipsoids, even for low axial ratio, and this function provides a precise method for characterizing the axial ratio of relatively symmetrical particles.

Besides its greater sensitivity than the β function (or the Ψ function), R has several other advantages:

(1) unlike β computation of R does not require knowledge of the absolute solute concentration (Rowe, 1977)

(2) less data is required to compute R and hence the error in the final function is minimized. As rotational parameters are generally very difficult to determine, as will be evident from the earlier parts of this chapter, the R function is also to be preferred over swelling independent functions involving these. The R function is also to be preferred over the scattering γ and α functions mainly because of the particle homogeneity problem mentioned in section 1.6. The β function can still however be useful, precisely because of its lack of variation for oblate ellipsoids, in deciding whether the macromolecule is better modelled by either a prolate or an oblate ellipsoid. Experimental values for β and $k_s/[\eta]$ ($\equiv$R) have been tabulated for a wide range of proteins by Creeth & Knight (1965). Values of β below the theoretical minimum of 2.112×10^6 and above 1.6 for R may indicate that some proteins cannot be modelled by an equivalent ellipsoid of revolution. This has been suggested for Bovine serum albumin (BSA). A table of values of axial ratio calculated from the R function for recent data, together with a comparison of their 'model dependent' estimates for $\bar{v}_s/\bar{v}$ with their 'model independent' estimates to determine the 'goodness of fit' of an ellipsoid of revolution, is given in Table 2.

1.8. Comment

Although a hydrodynamically equivalent ellipsoid of revolution model can now be fitted with much greater precision to many rigid macromolecules with the aid of the R function (and possibly the Π function)

the distinction still has to be made as to whether the macromolecule is better modelled either by a prolate or an oblate model. It is clear from a perusal of the crystallographic models of many globular proteins such as carboxypeptidase, myoglobin and ribonuclease (Table 3) that in many cases this is quite arbitrary and indeed in some cases is impossible

It would be a significant step forward therefore if the restriction of two equal axes on the ellipsoid were removed to allow use of the more general tri-axial ellipsoid. However, either due to the lack of the theoretical relationships linking the axial dimensions of the ellipsoid with experimental parameters, or, even if they are available, due to the lack of the necessary experimental precision, numerical inversion procedures or data analysis techniques, this model has not, to date, been available. The aim of the rest of this thesis is to show that the general tri-axial ellipsoid can now be successfully employed to model biological macromolecules in solution. We will start by deriving the tri-axial viscosity increment equation.

Table 1. Values of Λ, ε_a, ε_b, κ_1, κ_2, κ_3, ξ_1, ξ_2, ξ_3 and Π for prolate and oblate ellipsoids of revolution

axial ratio	1	2	3	4	5	6	7	8	9	10
Λ_p	2.500	2.490	2.692	3.071	3.575	4.177	4.862	5.624	6.457	7.359
Λ_o	2.500	2.356	2.187	2.070	1.989	1.931	1.887	1.854	1.827	1.805
$\varepsilon_{a,p}$	2.500	1.932	1.574	1.373	1.251	1.171	1.115	1.075	1.044	1.020
$\varepsilon_{a,o}$	2.500	2.522	2.343	2.202	2.102	2.029	1.974	1.931	1.896	1.868
$\varepsilon_{b,p}$	2.500	2.768	3.250	3.920	4.737	5.679	6.736	7.899	9.164	10.528
$\varepsilon_{b,o}$	2.500	2.273	2.110	2.003	1.932	1.882	1.844	1.815	1.792	1.774
$\kappa_{1,p}$	2.500	1.932	1.574	1.373	1.251	1.171	1.115	1.075	1.044	1.020
$\kappa_{1,o}$	2.500	2.522	2.343	2.202	2.102	2.029	1.974	1.931	1.896	1.868
$\kappa_{2,p}$	2.500	2.211	2.133	2.222	2.413	2.674	2.989	3.349	3.751	4.189
$\kappa_{2,o}$	2.500	2.439	2.265	2.136	2.045	1.980	1.930	1.892	1.862	1.837
$\kappa_{3,p}$	2.500	3.047	3.809	4.769	5.899	7.182	8.609	10.174	11.871	13.698
$\kappa_{3,o}$	2.500	2.190	2.032	1.937	1.875	1.832	1.801	1.777	1.758	1.742
$\xi_{1,p}$	1.000	0.756	0.588	0.487	0.421	0.374	0.340	0.313	0.292	0.275
$\xi_{1,o}$	1.000	1.000	0.920	0.860	0.818	0.787	0.763	0.745	0.731	0.719
$\xi_{2,p}$	1.000	0.865	0.797	0.788	0.811	0.854	0.911	0.976	1.051	1.129
$\xi_{2,o}$	1.000	0.967	0.890	0.834	0.796	0.768	0.747	0.731	0.718	0.707
$\xi_{3,p}$	1.000	1.192	1.423	1.691	1.983	2.295	2.623	2.966	3.322	3.690
$\xi_{3,o}$	1.000	0.868	0.798	0.757	0.729	0.711	0.697	0.686	0.678	0.671
Π_p	3.200	3.122	2.960	2.778	2.601	2.438	2.291	2.159	2.041	1.935
Π_o	3.200	3.180	3.179	3.192	3.208	3.225	3.241	3.255	3.268	3.280

subscript p: prolate ellipsoid

o: oblate ellipsoid

Table 2. Use of the R function to predict the conformation of various macromolecules in solution in terms of an ellipsoid of revolution model

Protein	k_s ml/gm	k_η ml/gm	$[\eta]$ ml/gm	R	axial ratio	model dependent $(\bar{\nu}_s/\bar{\nu})$	model independent $(\bar{\nu}_s/\bar{\nu})$	Conclusion
Apoferritin[1]	8	12	5.16	1.55	1.45* †	2.6* †	1.5	spherical
BSA[2]	5.5	7.7	2.75	2.0	—	—	1.4	not a hydrodynamic ellipsoid (cf $\beta <$ 2.1)
Fibrinogen[3]	7	14	7.8	0.9	6.3†	1.1†	2.0	prolate ellipsoid ~6:1. Agrees with electron microscopy (Hall & Slayter, 1959)
C-protein[4]	11	15.4	12.6	0.87	26.0*, 6.65†	0.9*, 2.12†	1.4	oblate ellipsoid ~25:1
Myosin[5]	85	92	234	0.38	30†	4.3†	1.1	not hydrodynamic ellipsoids of revolution
Synthetic A-filaments[6]	160.8	366	176	0.9	19.5†	16†	2.3	
Collagen sonicates[7]								
(i) M_r = 352,000	308	880	1252	0.246	80†	2.28†	2.85	prolate ~80:1
(ii) M_r = 330,000	291	756	1078	0.270	64†	2.85†	2.60	prolate ~65:1
(iii) M_r = 273,000	241	564	639	0.377	30†	6.12†	2.34	not hydrodynamic ellipsoids of revolution
(iv) M_r = 227,000	193	428	400	0.483	18†	9.13†	2.22	

† prolate ellipsoid, * oblate ellipsoid. Refs: 1&2 Rowe & Pancholi (unpub.), 3 Rowe & Mihalyi (unpub.) 4 Offer et al (1973), 5 Emes (1977), Emes & Rowe (1978a), 6 Emes (1977), Emes & Rowe (1978b), 7 from Nisihara & Doty (1958)

Table 3. Crystallographic dimensions of some globular proteins

Protein	Dimensions (Å)	Reference
Carboxypeptidase	50 x 42 x 38	Lipscomb (1971)
Myoglobin	43 x 35 x 23	Kendrew et al (1958)
Cytochrome c	25 x 25 x 35	Dickerson & Geiss (1969)
Lysosyme	45 x 30 x 30	Blake et al (1965)
Ribonuclease	38 x 28 x 22	Kartha et al (1967)
Pre - albumin	70 x 55 x 50	Blake et al (1978)
Hemoglobin	64 x 55 x 50	Perutz et al (1960)

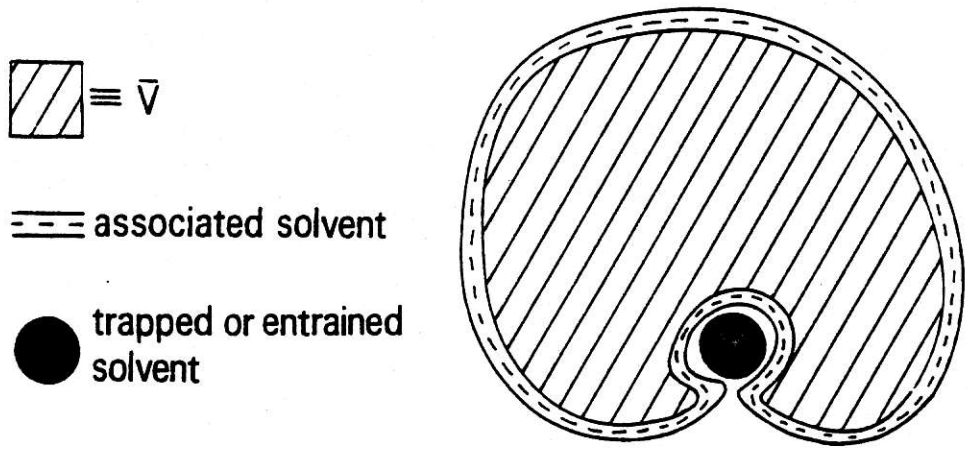

Figure 1. A macromolecule in solution is generally swollen due to solvent association

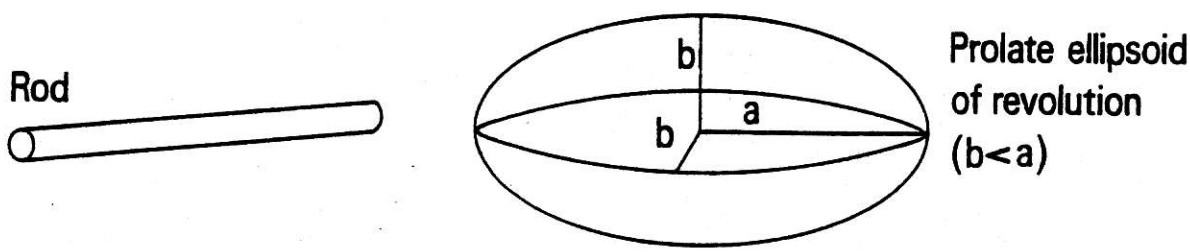

Figure 2. Mathematical models for macromolecules in solution

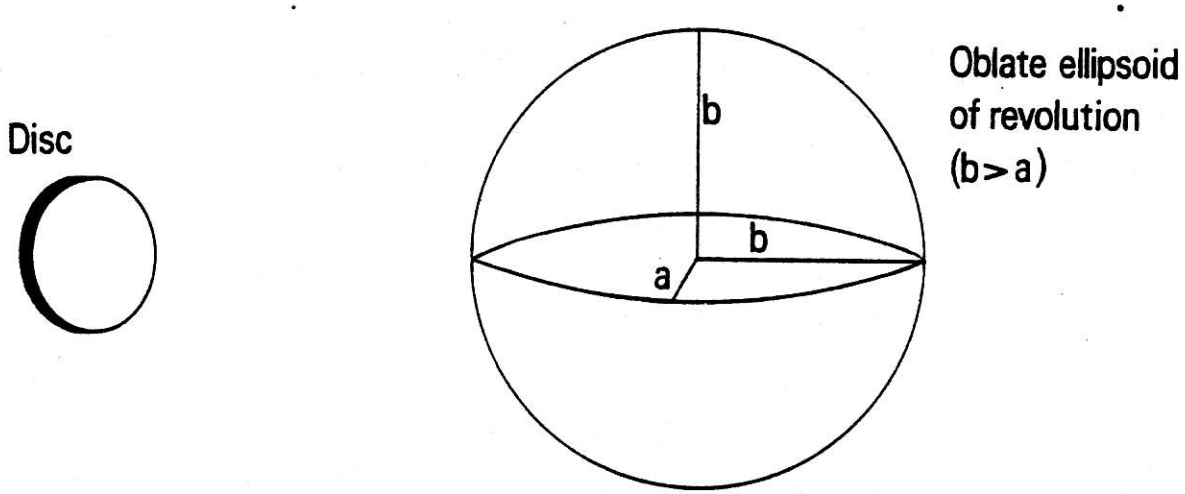

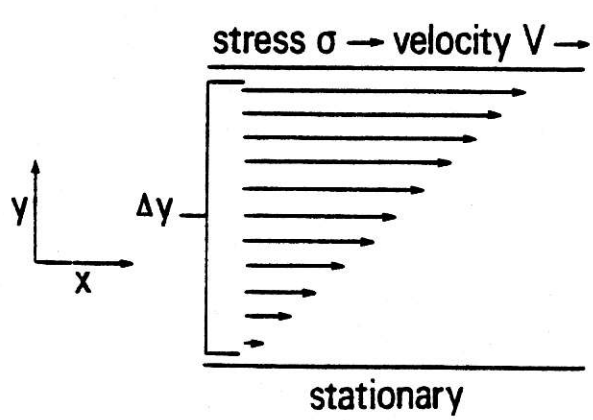

length of arrows are proportional to the fluid velocity at that value of y

Figure 3. Shearing of a Newtonian fluid between parallel plates (from Van Holde, 1971)

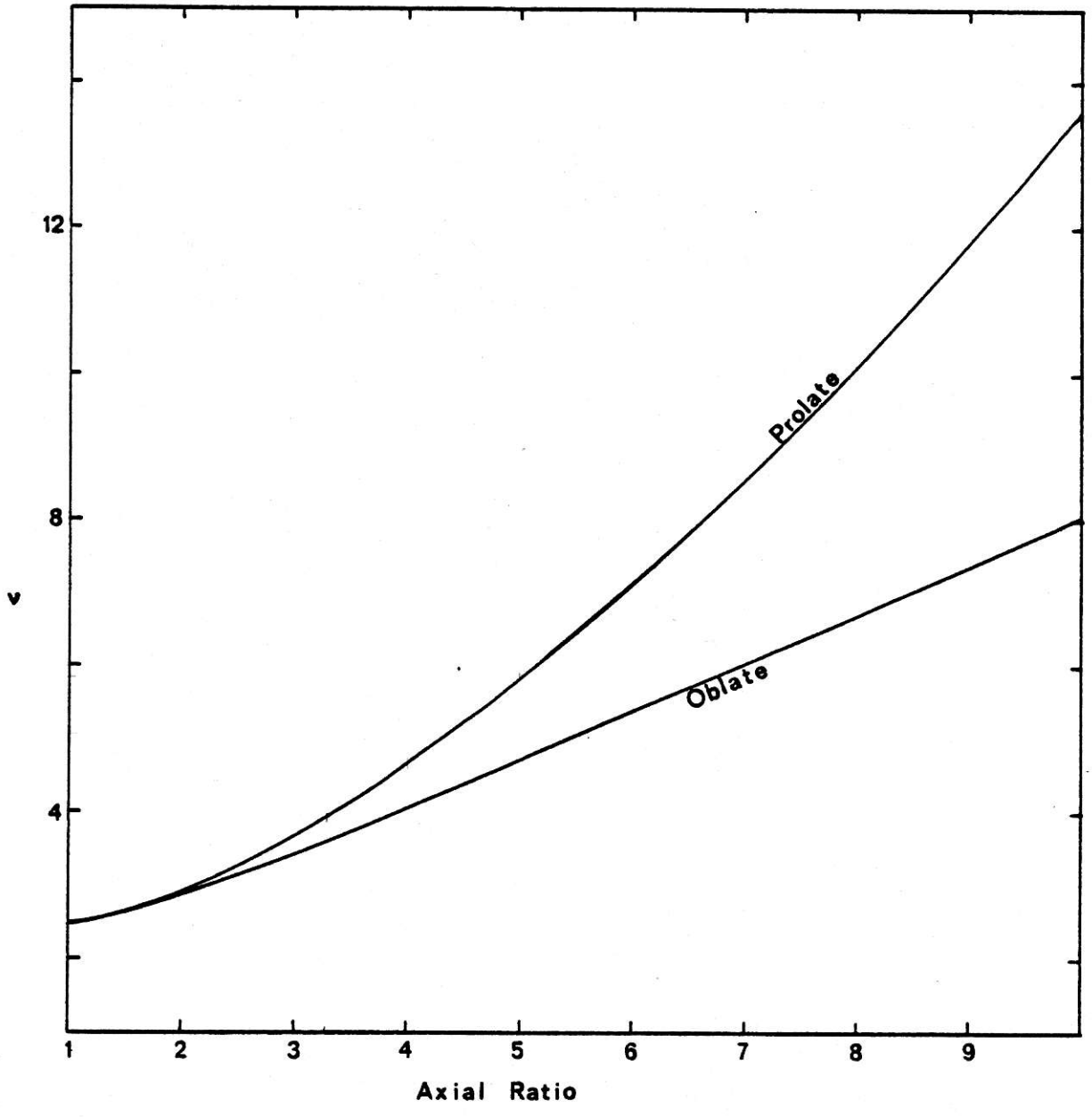

Figure 4. Plot of the viscosity increment as a function of axial ratio for ellipsoids of revolution

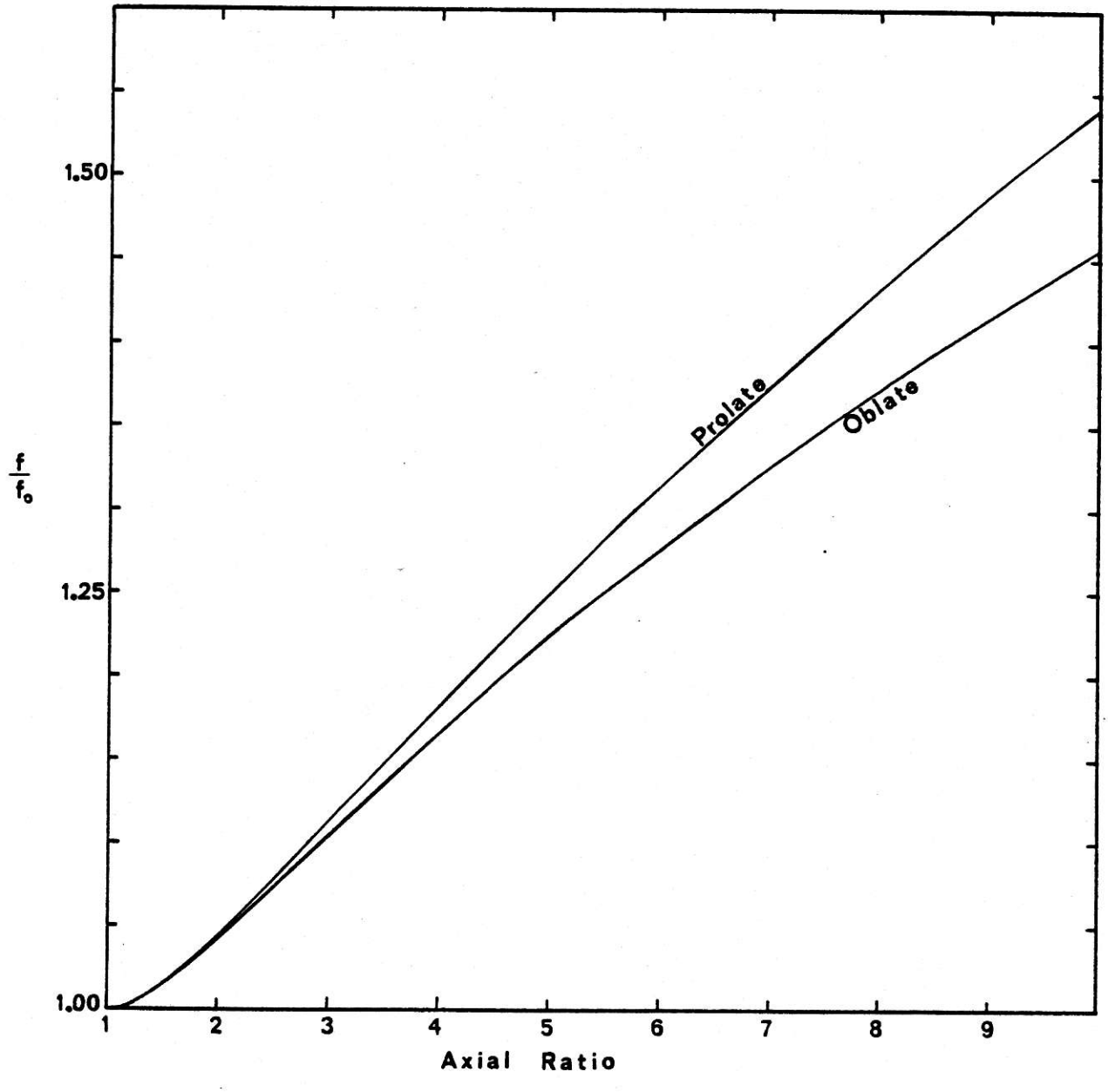

Figure 5. Plot of the translational frictional ratio (the "Perrin function") as a function of axial ratio for ellipsoids of revolution

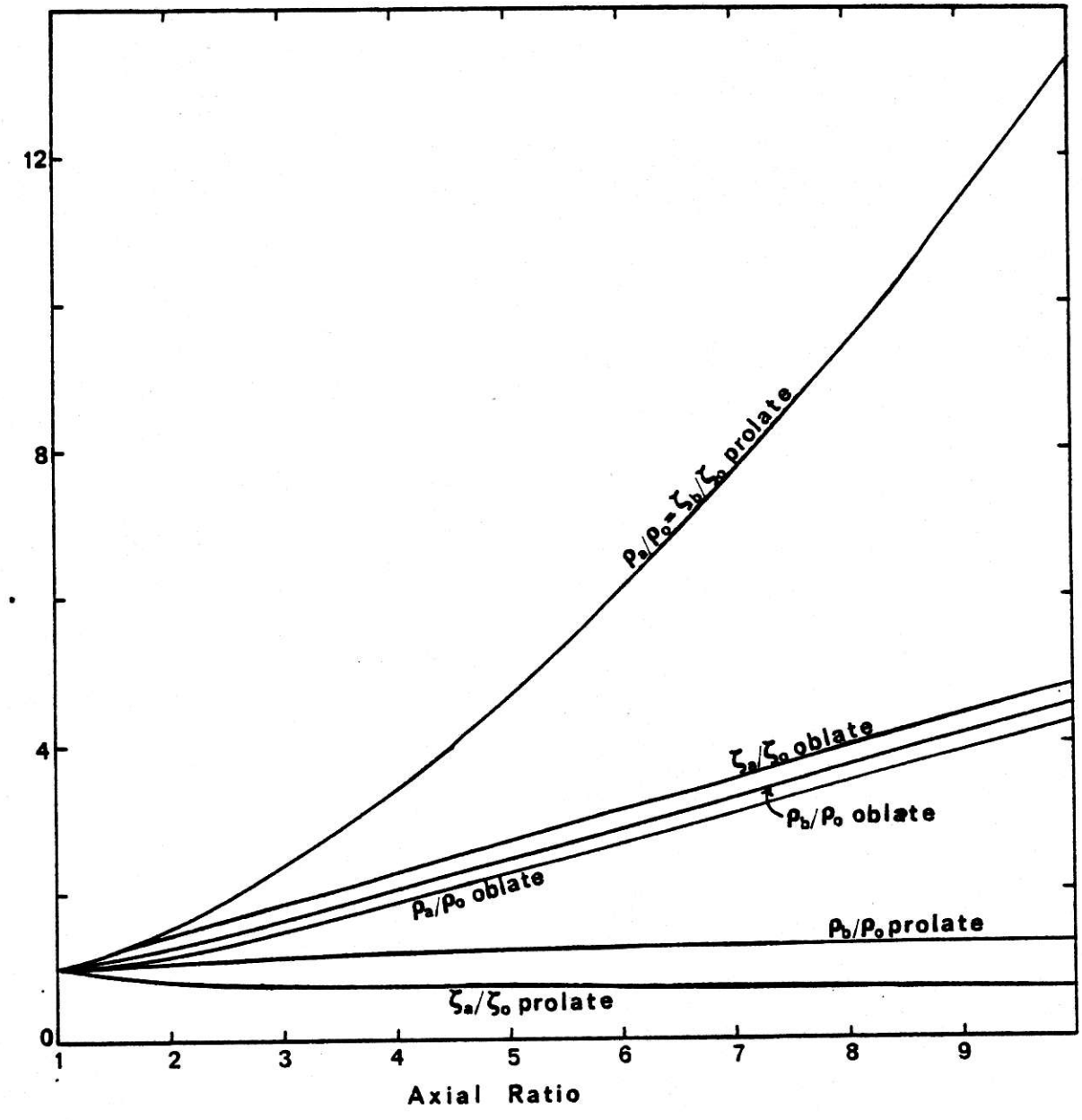

Figure 6. Plot of the rotational diffusion coefficient ratios and rotational relaxation time ratios as a function of axial ratio for ellipsoids of revolution

Figure 7. Dielectric dispersion curves for prolate ellipsoids of revolution. Constant dipole angle ($\theta = 45^{o}$) and varying axial ratio (a/b from 1 to 50). From Oncley (1940)

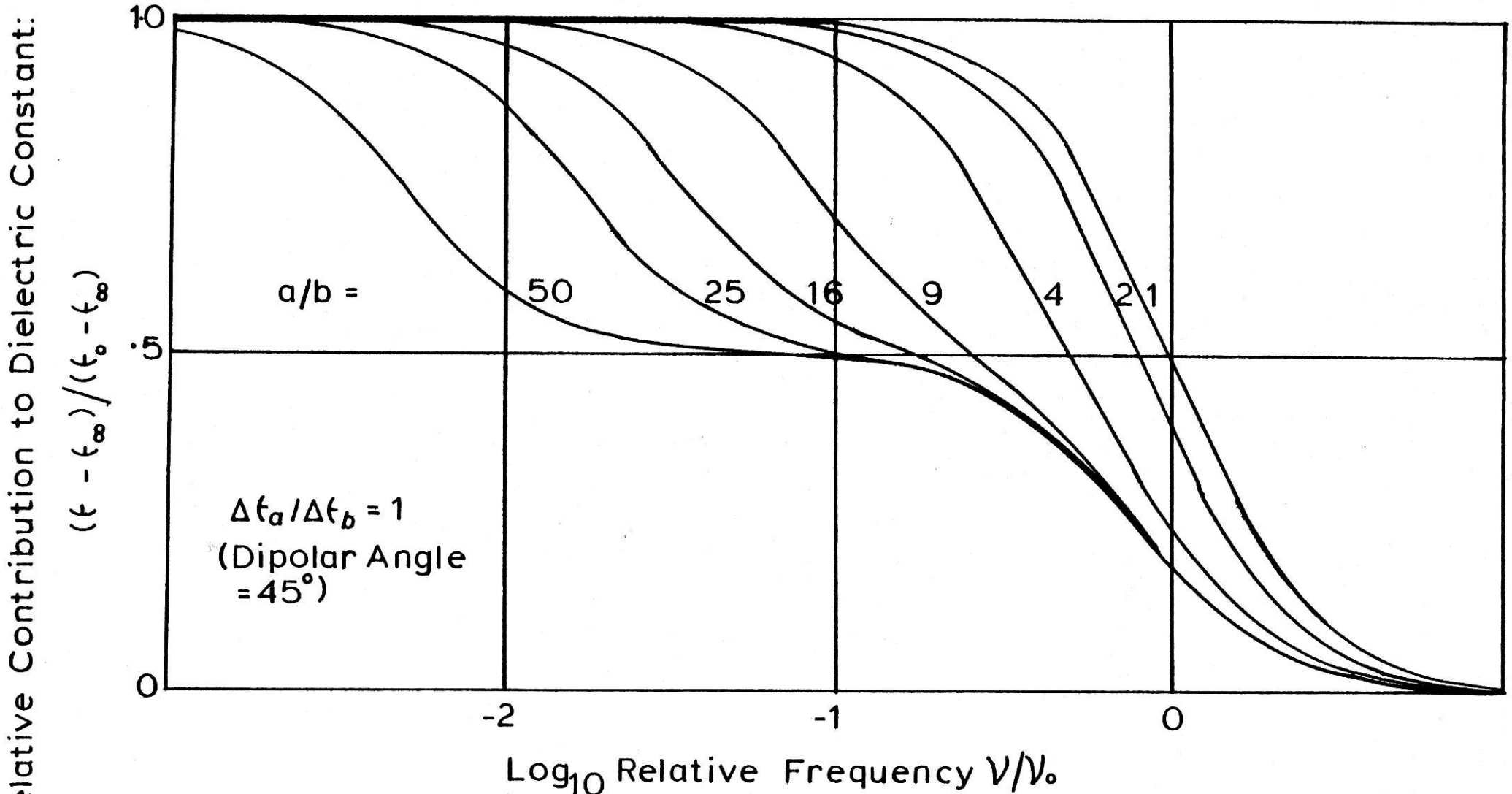
Relative Contribution to Dielectric Constant:
$(\epsilon - \epsilon_\infty)/(\epsilon_o - \epsilon_\infty)$
1·0
·5
0
a/b =
50
25
16
9
4
2
1
$\Delta\epsilon_a/\Delta\epsilon_b = 1$
(Dipolar Angle
=45°)
-2
-1
0
Log_{10} Relative Frequency ν/ν_o

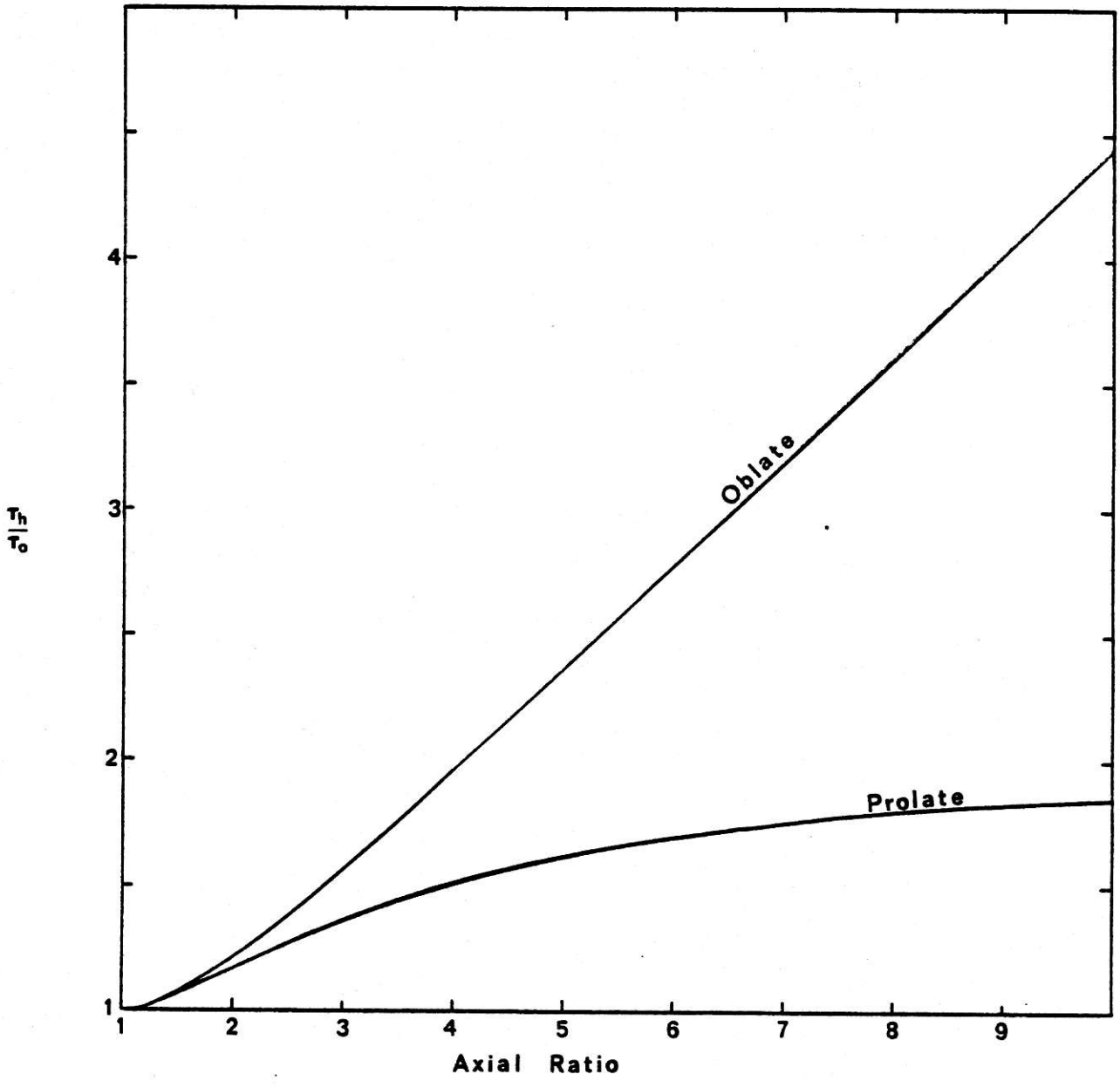

Figure 8. Plot of the harmonic mean rotational relaxation time ratio as a function of axial ratio for ellipsoids of revolution

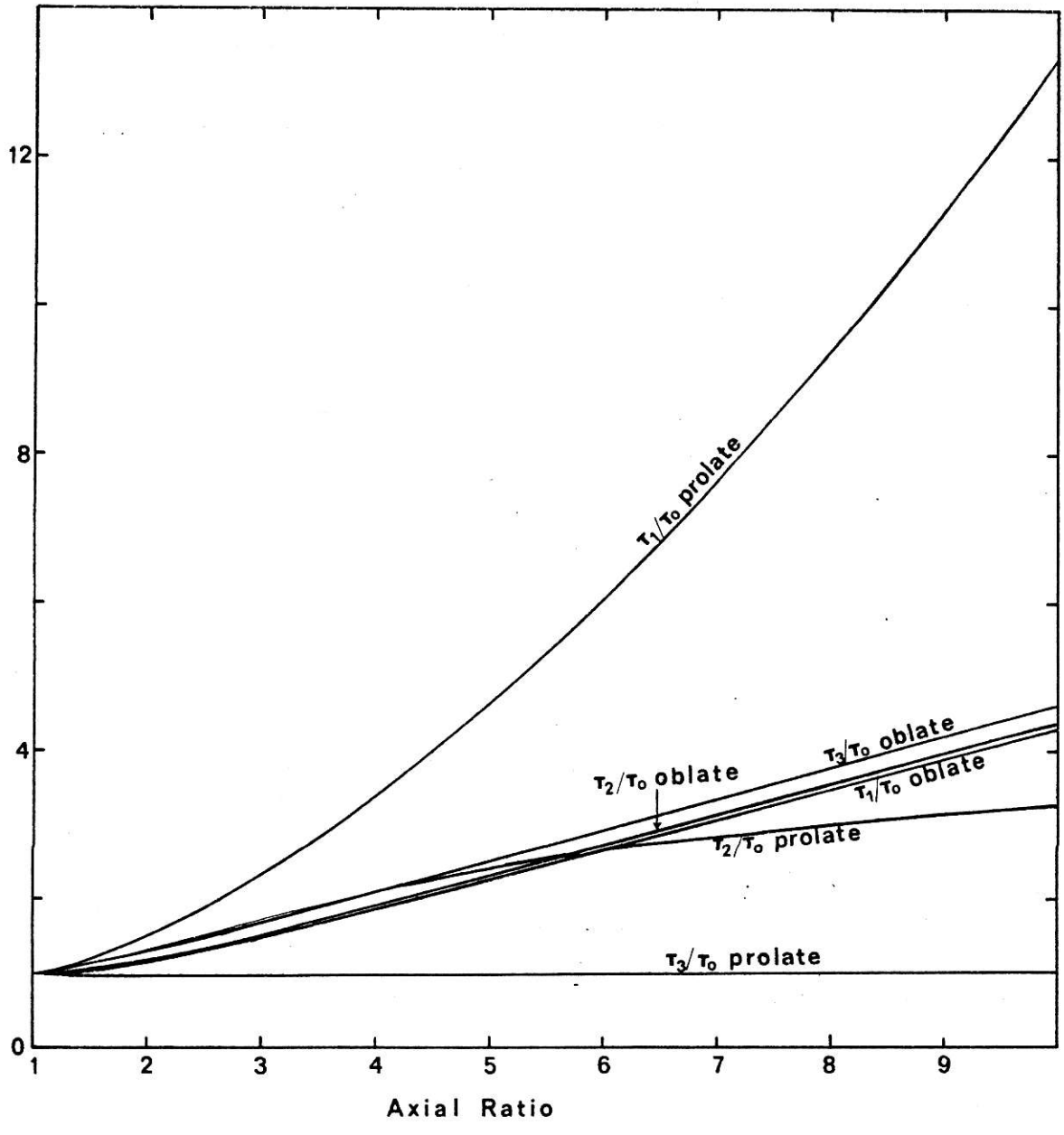

Figure 9. Plot of the fluorescence anisotropy relaxation time ratios as a function of axial ratio for ellipsoids of revolution

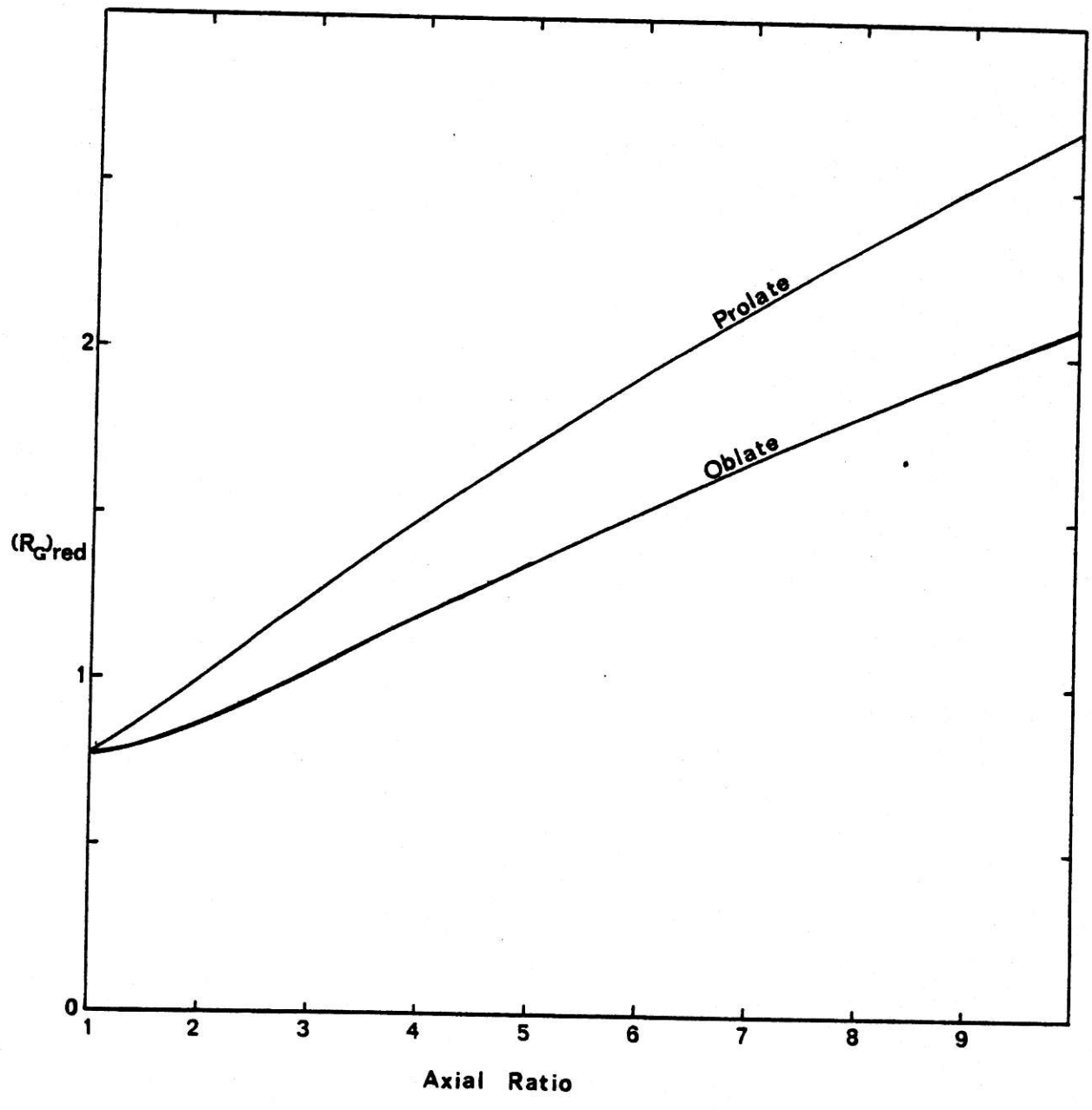

Figure 10. Plot of the 'reduced' radius of gyration as a function of axial ratio for ellipsoids of revolution

Figure 11. (a) Values of axial ratio and hydration as a function of $\nu(\bar{v}_s/\bar{v})$. Contour lines denote values of $\nu(\bar{v}_s/\bar{v})$

(b) As above, but as a function of $(f/f_0).(\bar{v}_s/\bar{v})^{1/3}$.

Contour lines denote values of $(f/f_0).(\bar{v}_s/\bar{v})^{1/3}$

(from Oncley, 1941)

(a)

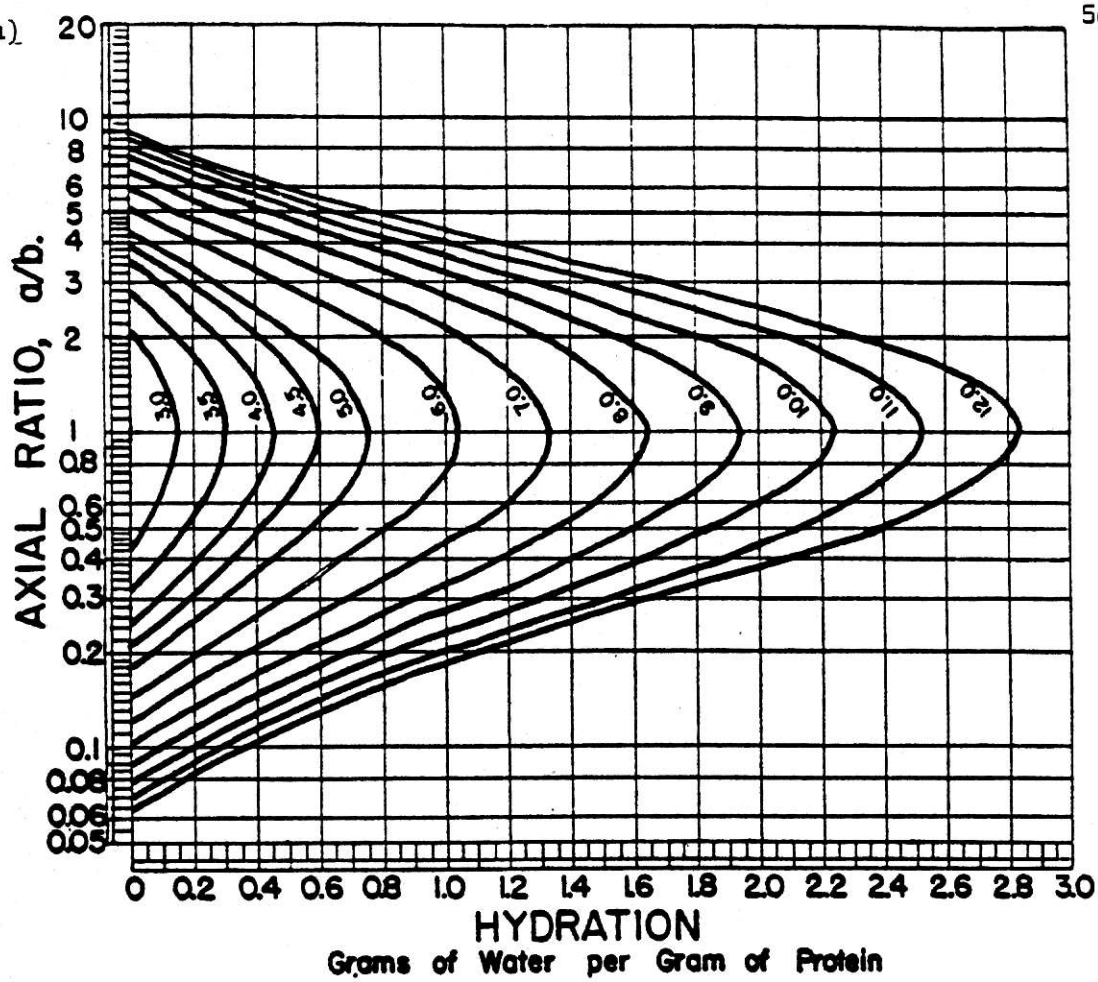
AXIAL RATIO, a/b.
20
10
8
6
5
4
3
2
1
0.8
0.6
0.5
0.4
0.3
0.2
0.1
0.08
0.06
0.05
3.0
3.5
4.0
4.5
5.0
6.0
7.0
8.0
9.0
10.0
11.0
12.0
0 0.2 0.4 0.6 0.8 1.0 1.2 1.4 1.6 1.8 2.0 2.2 2.4 2.6 2.8 3.0
HYDRATION
Grams of Water per Gram of Protein

(b)

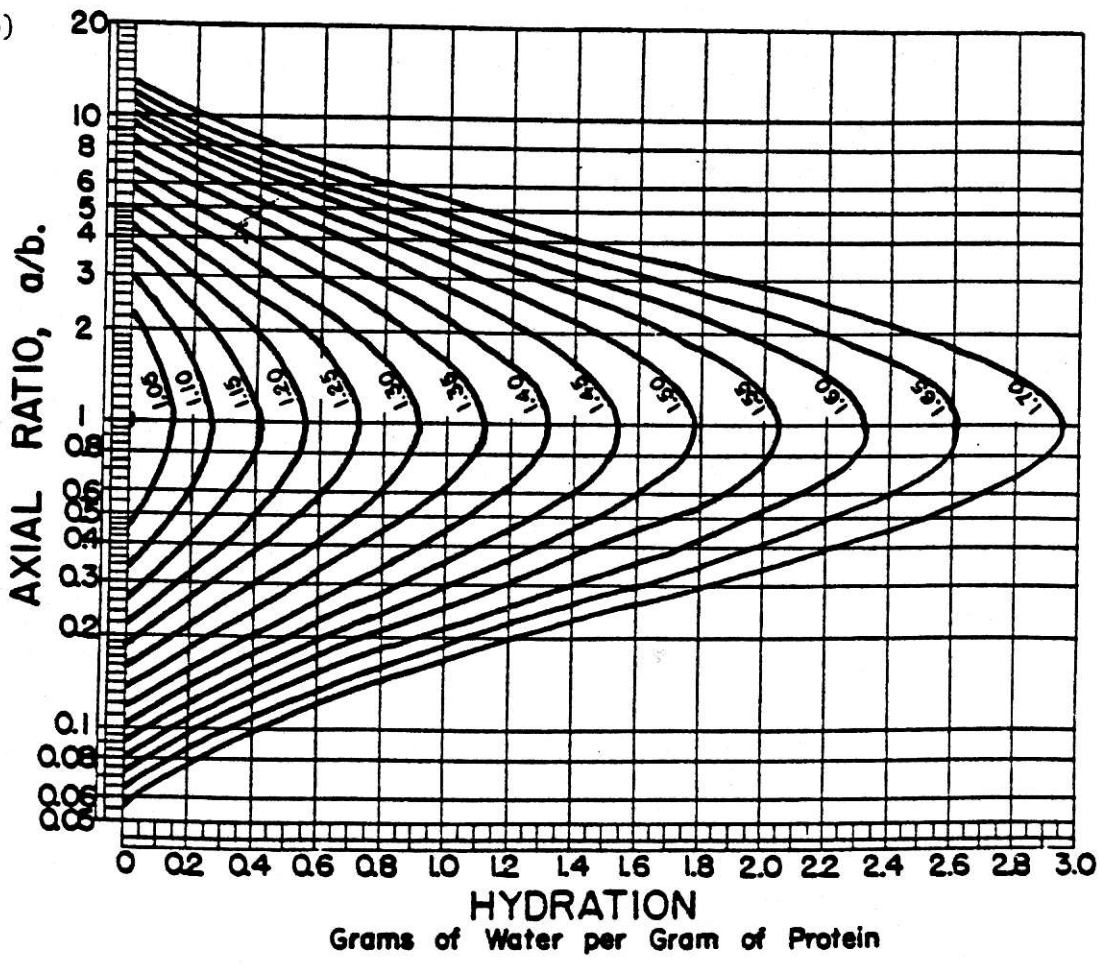
AXIAL RATIO, a/b.
20
10
8
6
5
4
3
2
1
0.8
0.6
0.5
0.4
0.3
0.2
0.1
0.08
0.06
0.05
1.05
1.10
1.15
1.20
1.25
1.30
1.35
1.40
1.45
1.50
1.55
1.60
1.65
1.70
0 0.2 0.4 0.6 0.8 1.0 1.2 1.4 1.6 1.8 2.0 2.2 2.4 2.6 2.8 3.0
HYDRATION
Grams of Water per Gram of Protein

Figure 12. Asymmetry and hydration (i.e. solvent association) of certain protein molecules. (from Oncley, 1941)

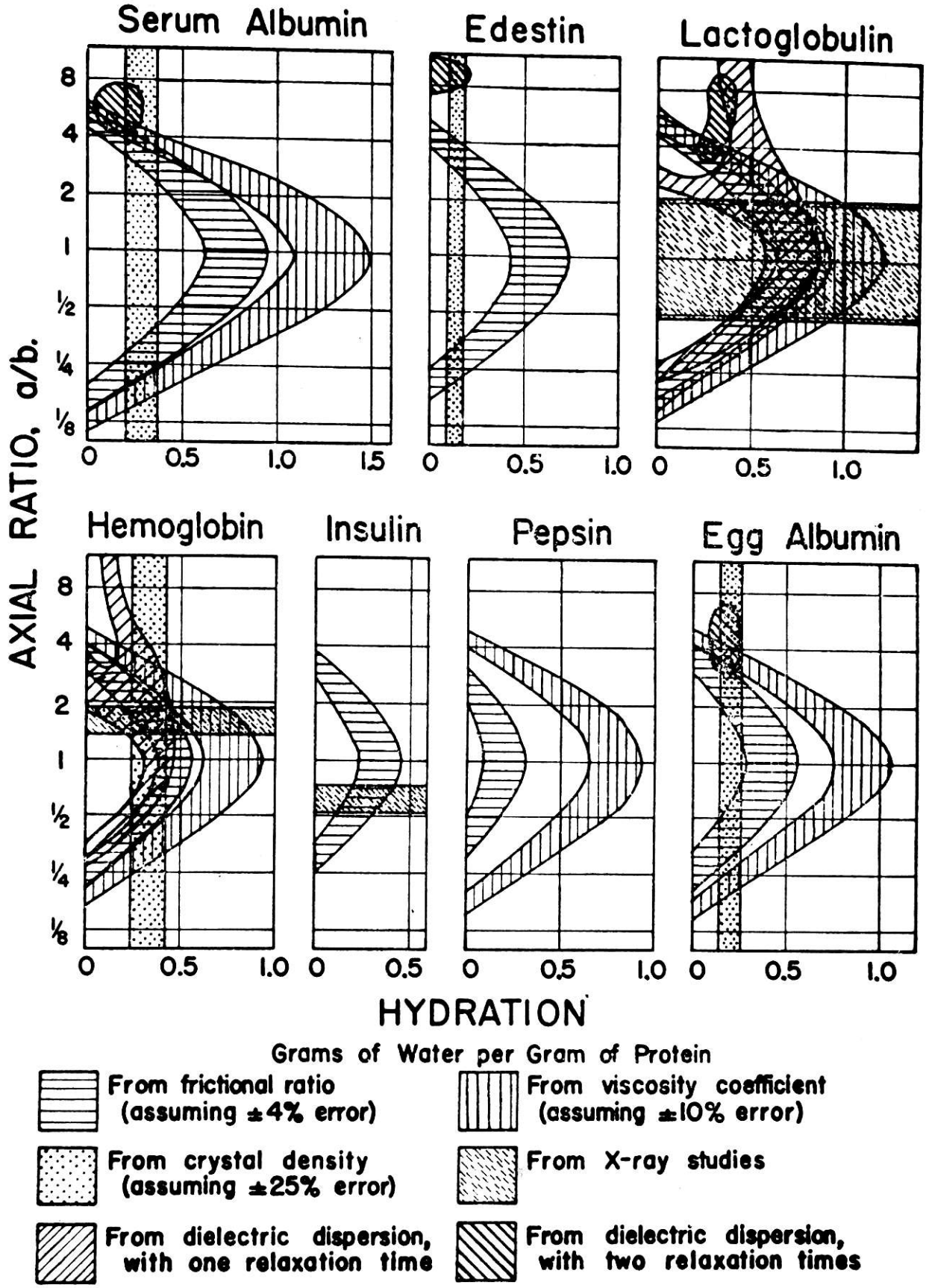
Serum Albumin
Edestin
Lactoglobulin
Hemoglobin
Insulin
Pepsin
Egg Albumin
AXIAL RATIO, a/b.
8
4
2
1
½
¼
⅛
0
0.5
1.0
1.5
HYDRATION
Grams of Water per Gram of Protein
From frictional ratio (assuming ±4% error)
From viscosity coefficient (assuming ±10% error)
From crystal density (assuming ±25% error)
From X-ray studies
From dielectric dispersion, with one relaxation time
From dielectric dispersion, with two relaxation times

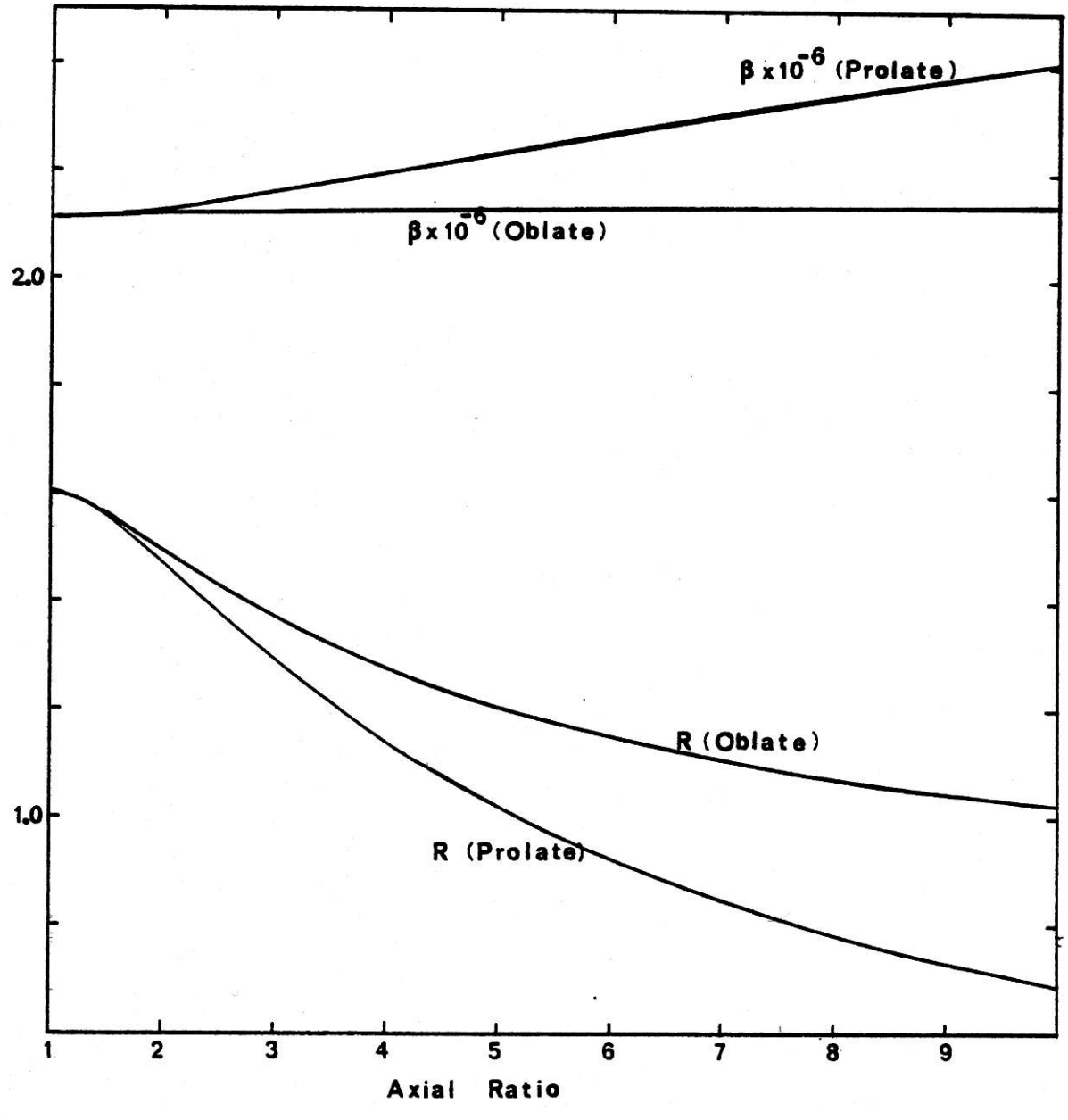

Figure 13. Plot of the Scheraga & Mandelkern β (x 10^{-6}) and Rowe R functions versus axial ratio for ellipsoids of revolution

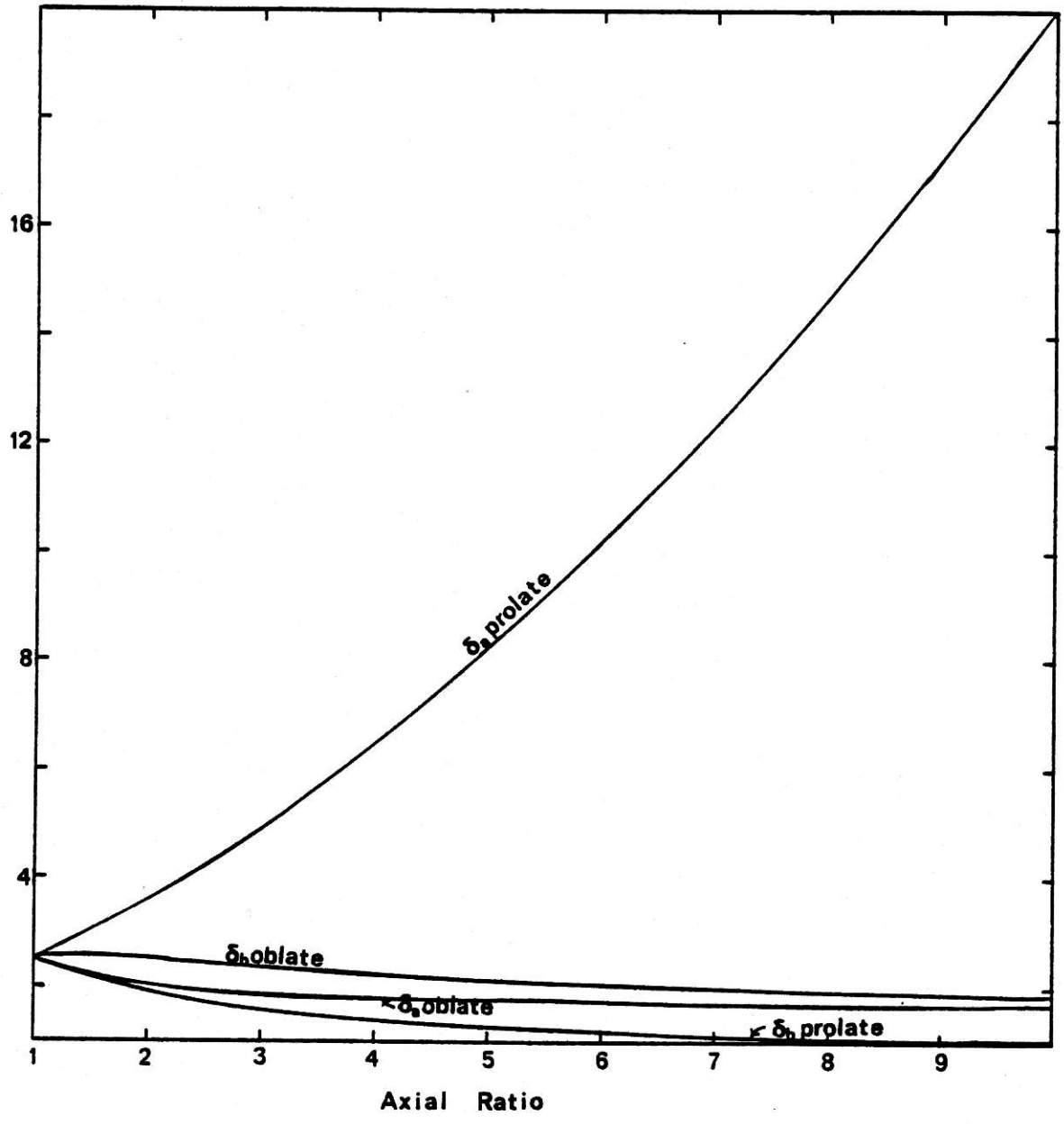

Figure 14. Plot of δ_a and δ_b as functions of axial ratio for ellipsoids of revolution

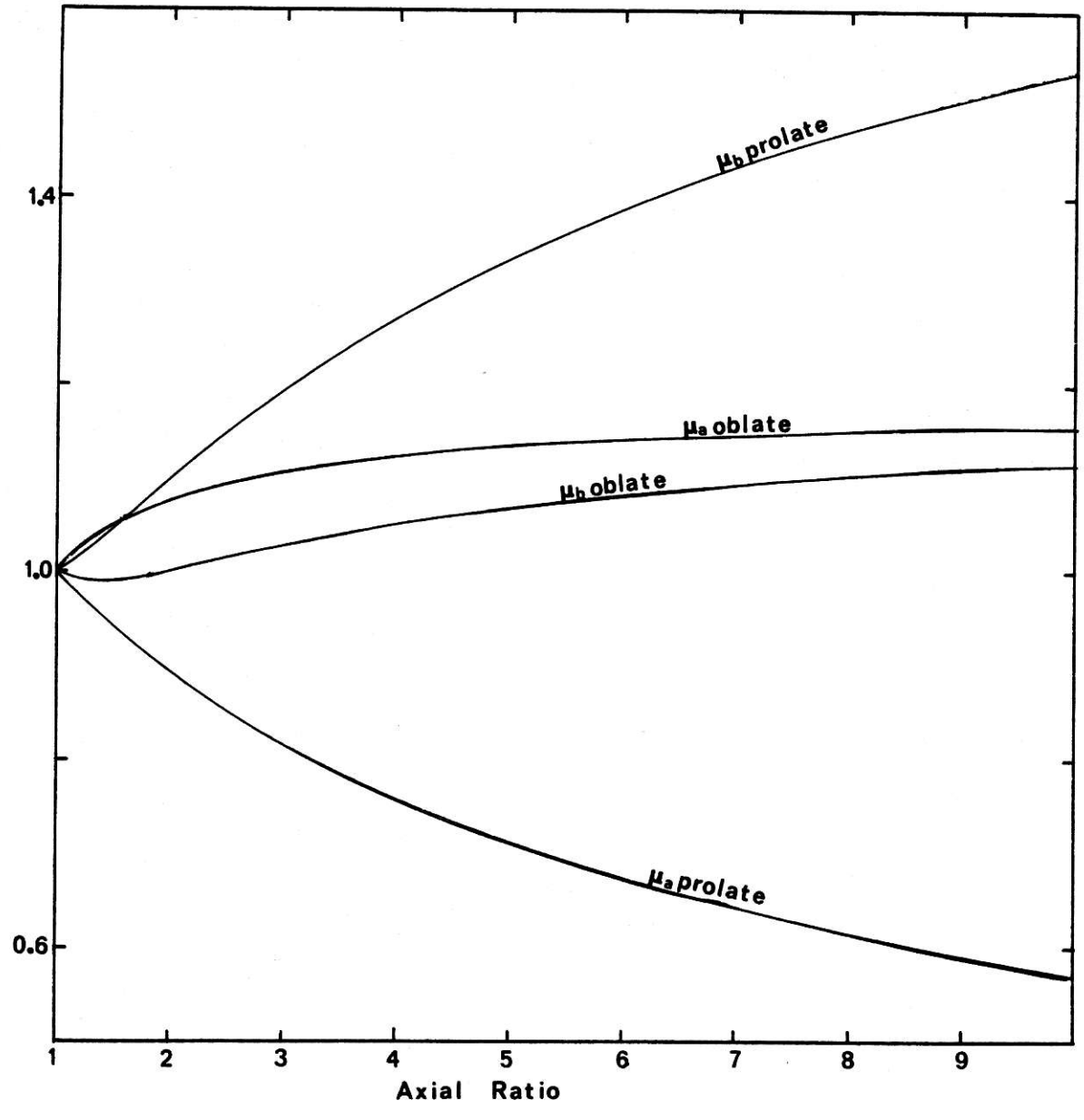

Figure 15. Plot of μ_a and μ_b as functions of axial ratio for ellipsoids of revolution

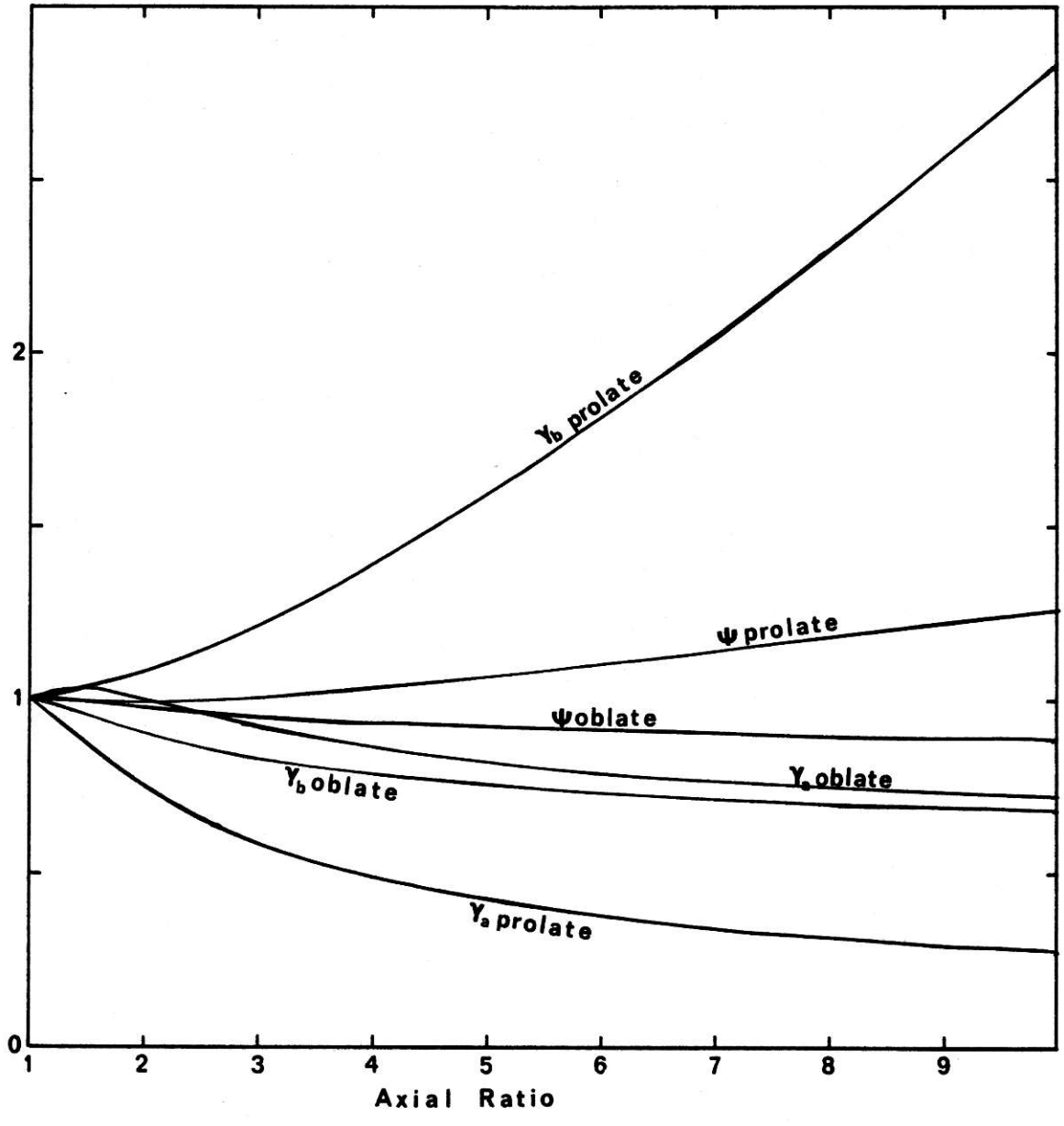

Figure 16. Plot of γ_a, γ_b and Ψ as functions of axial ratio for ellipsoids of revolution

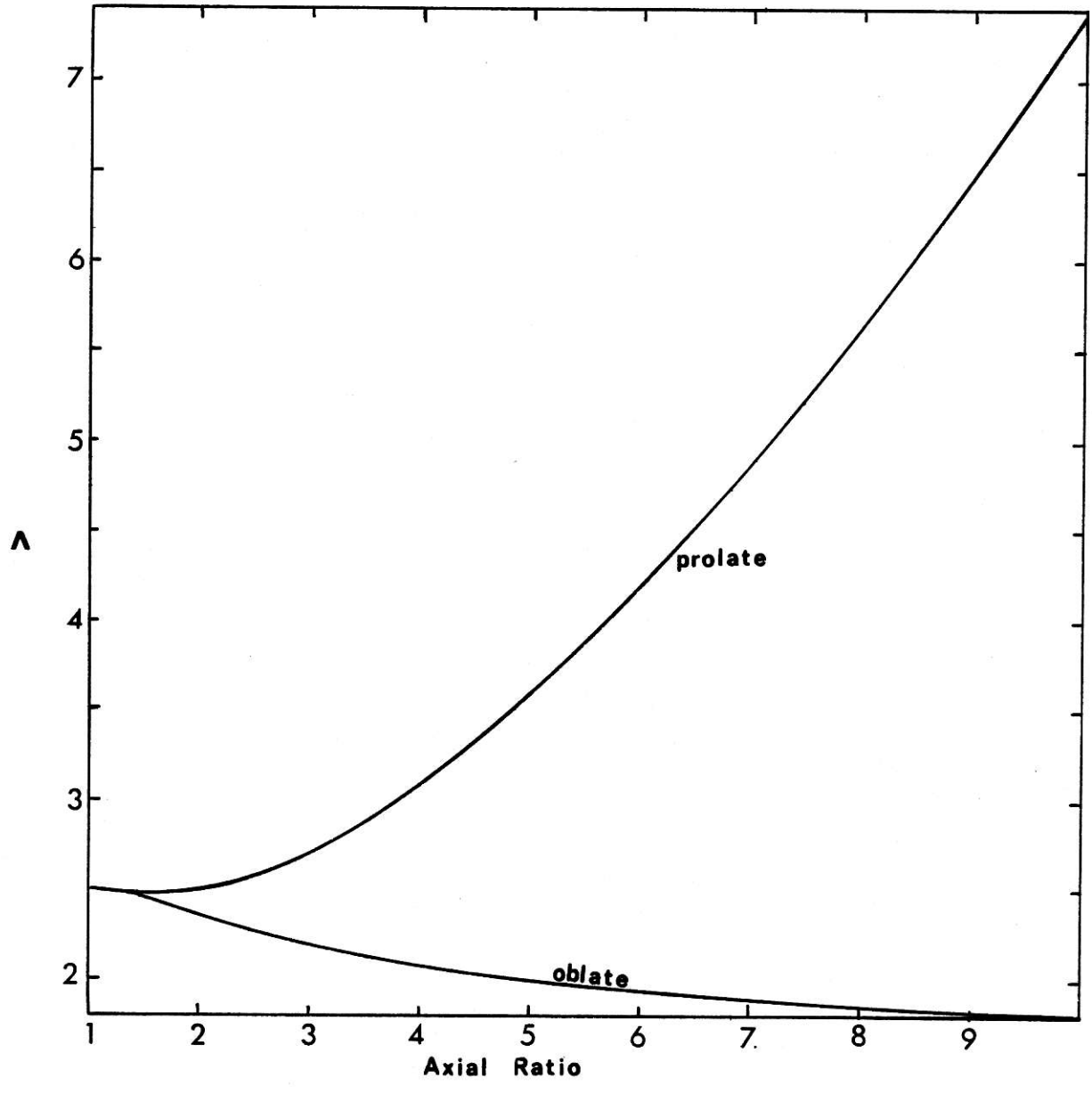

Figure 17. Plot of Λ as a function of axial ratio for ellipsoids of revolution

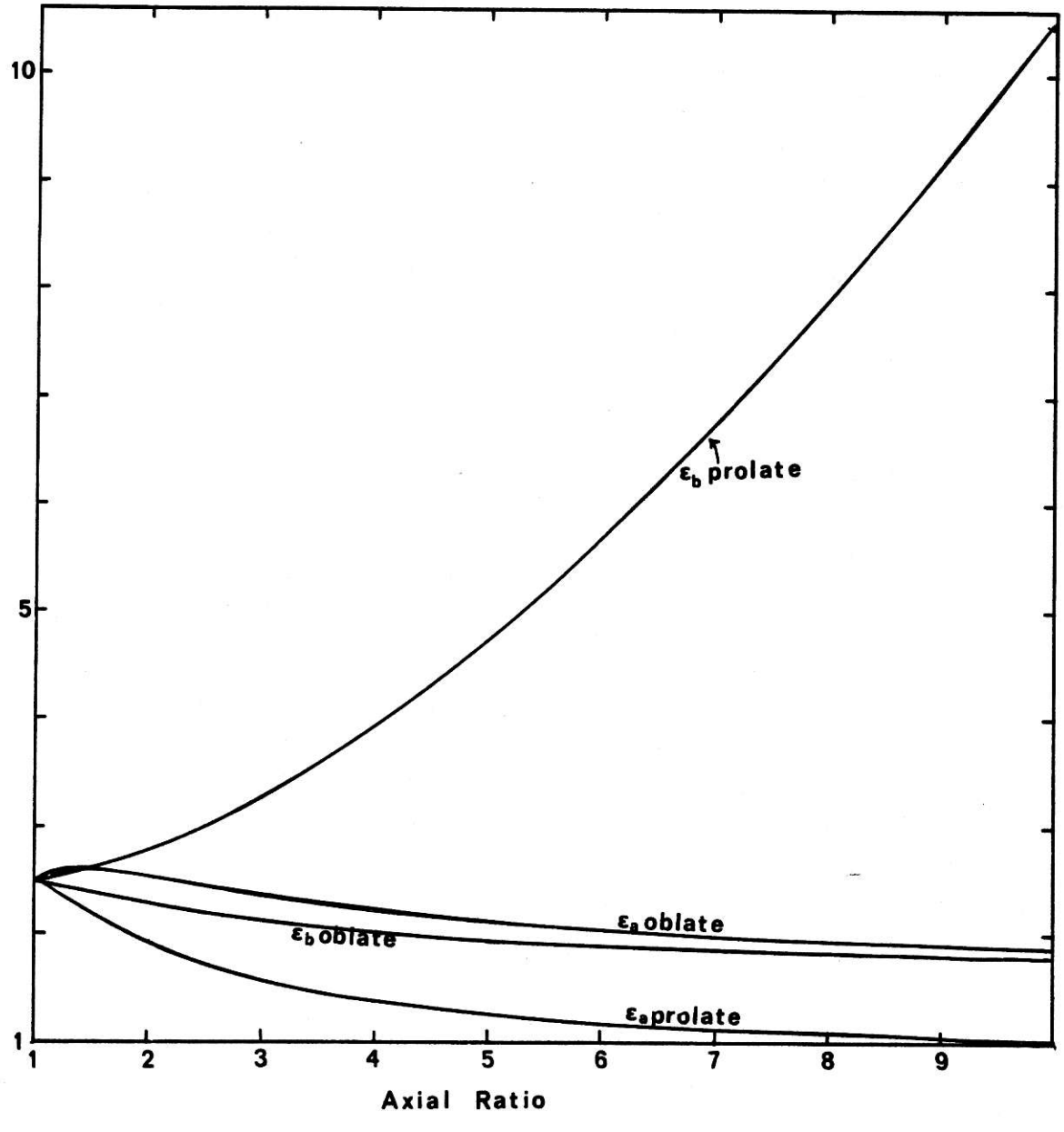

Figure 18. Plot of ε_a and ε_b as functions of axial ratio for ellipsoids of revolution

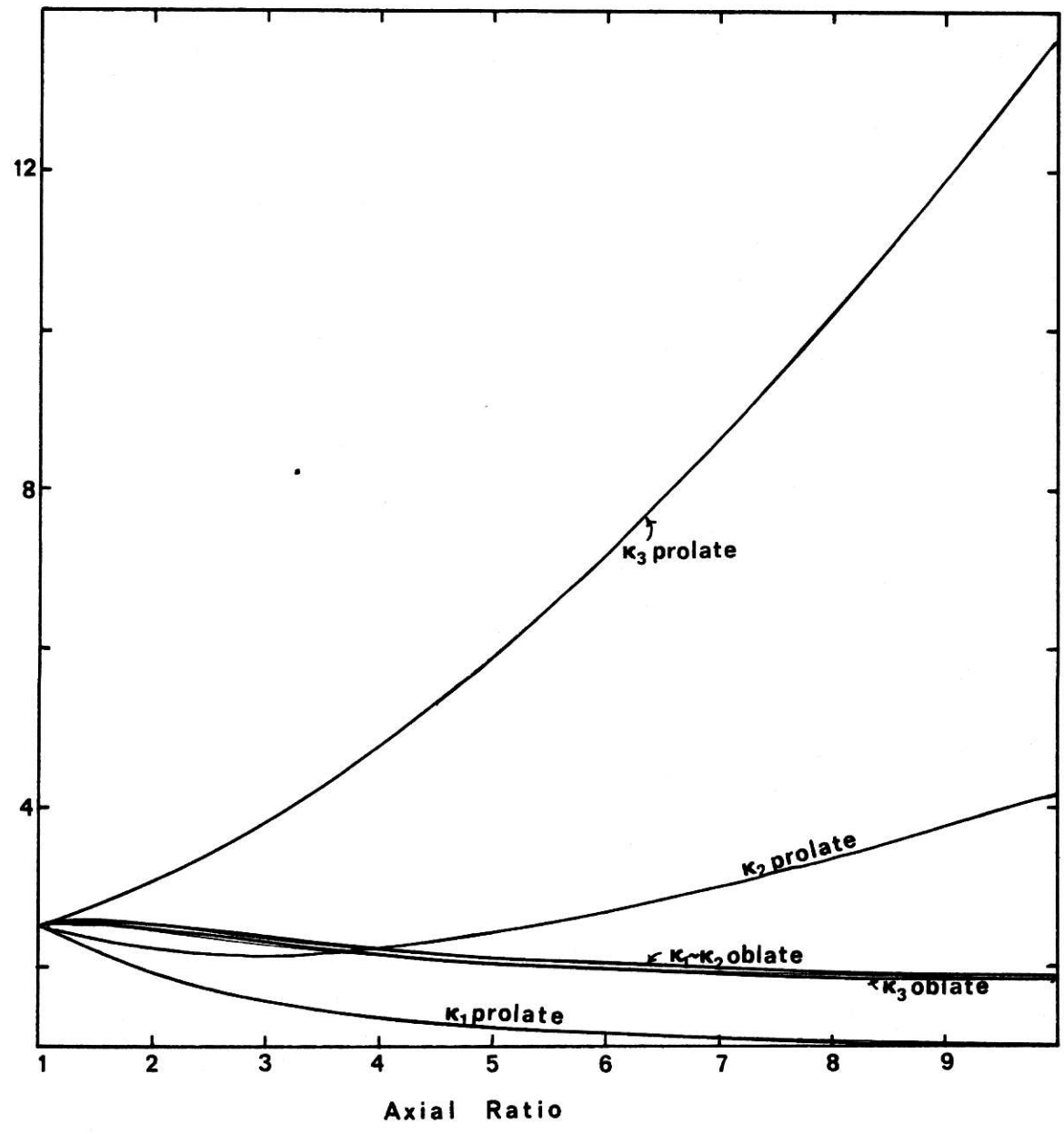

Figure 19. Plot of κ_1, κ_2 and κ_3 as functions of axial ratio for ellipsoids of revolution

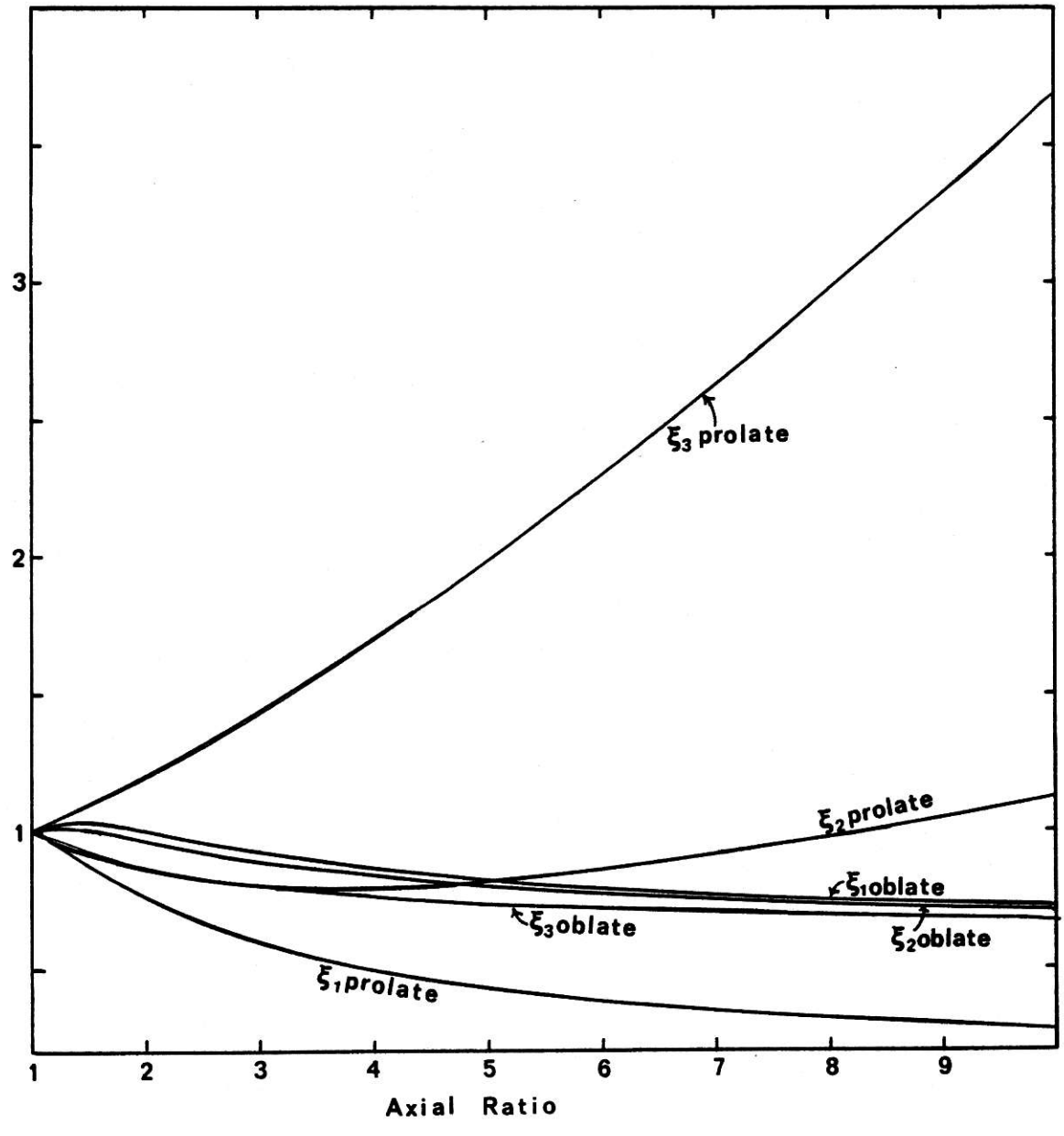

Figure 20. Plot of ξ_1, ξ_2 and ξ_3 as functions of axial ratio for ellipsoids of revolution

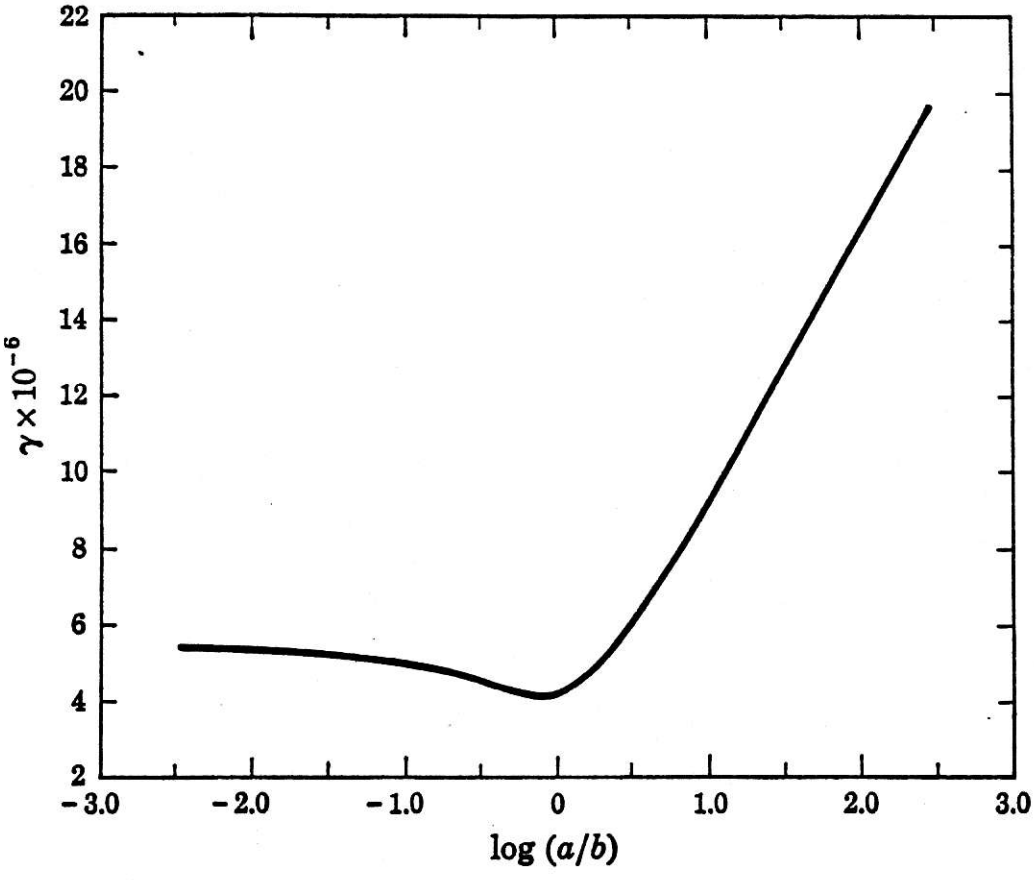

Figure 21. Plot of γ as a function of axial ratio for ellipsoids of revolution (from Martin, 1964)

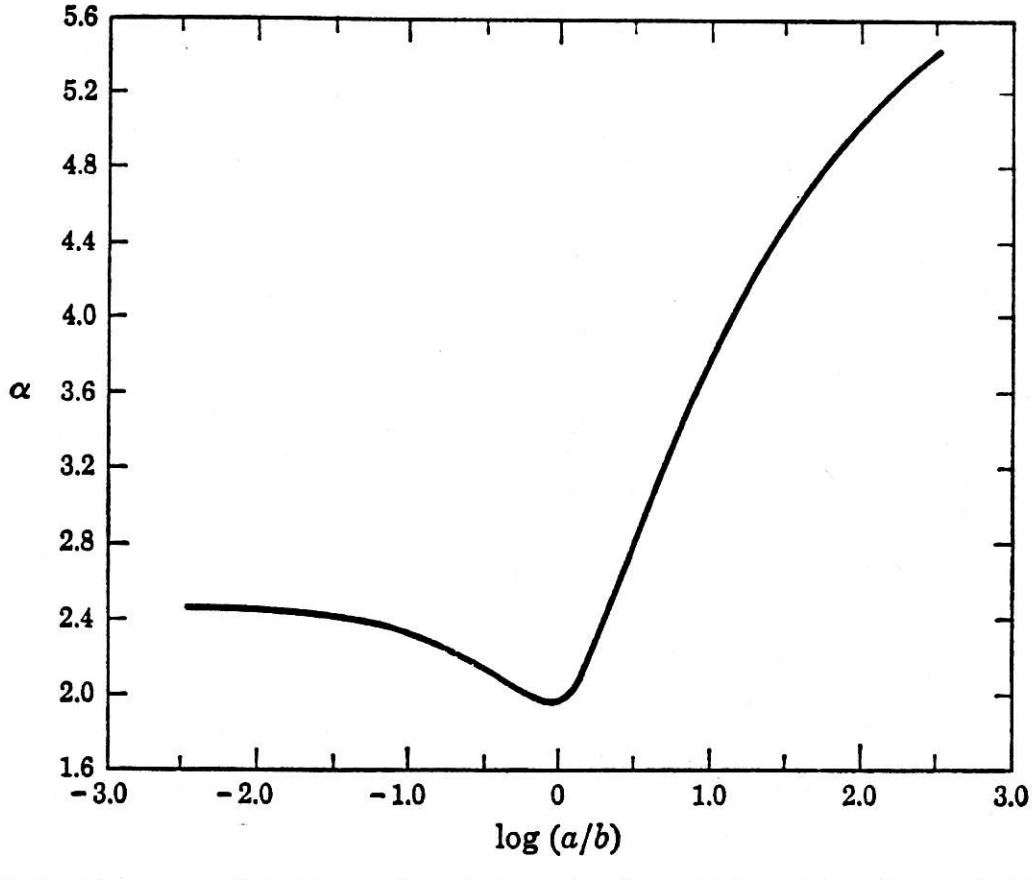

Figure 22. Plot of α as a function of axial ratio for ellipsoids of revolution

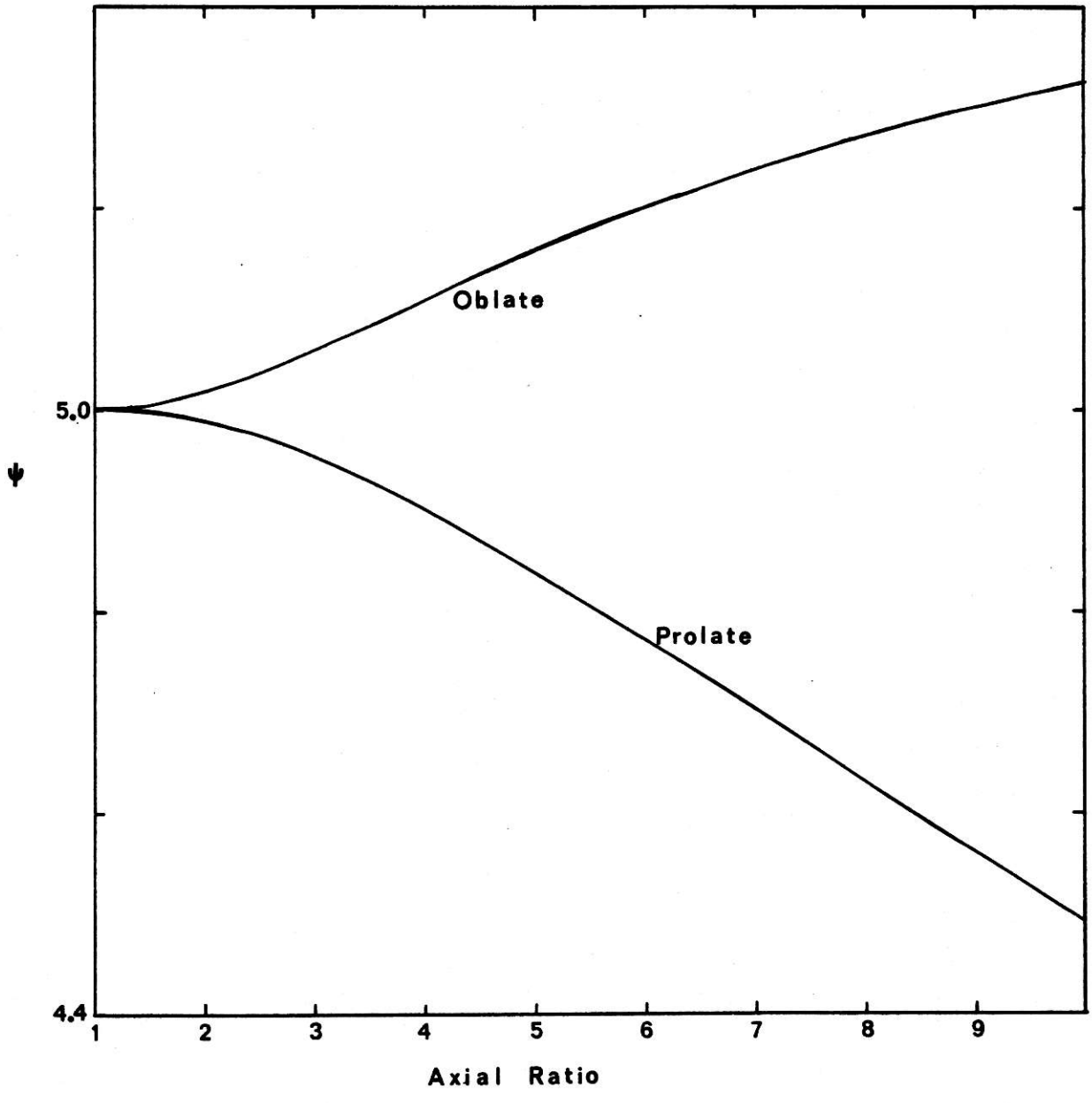

Figure 23. Plot of ψ as a function of axial ratio for ellipsoids of revolution

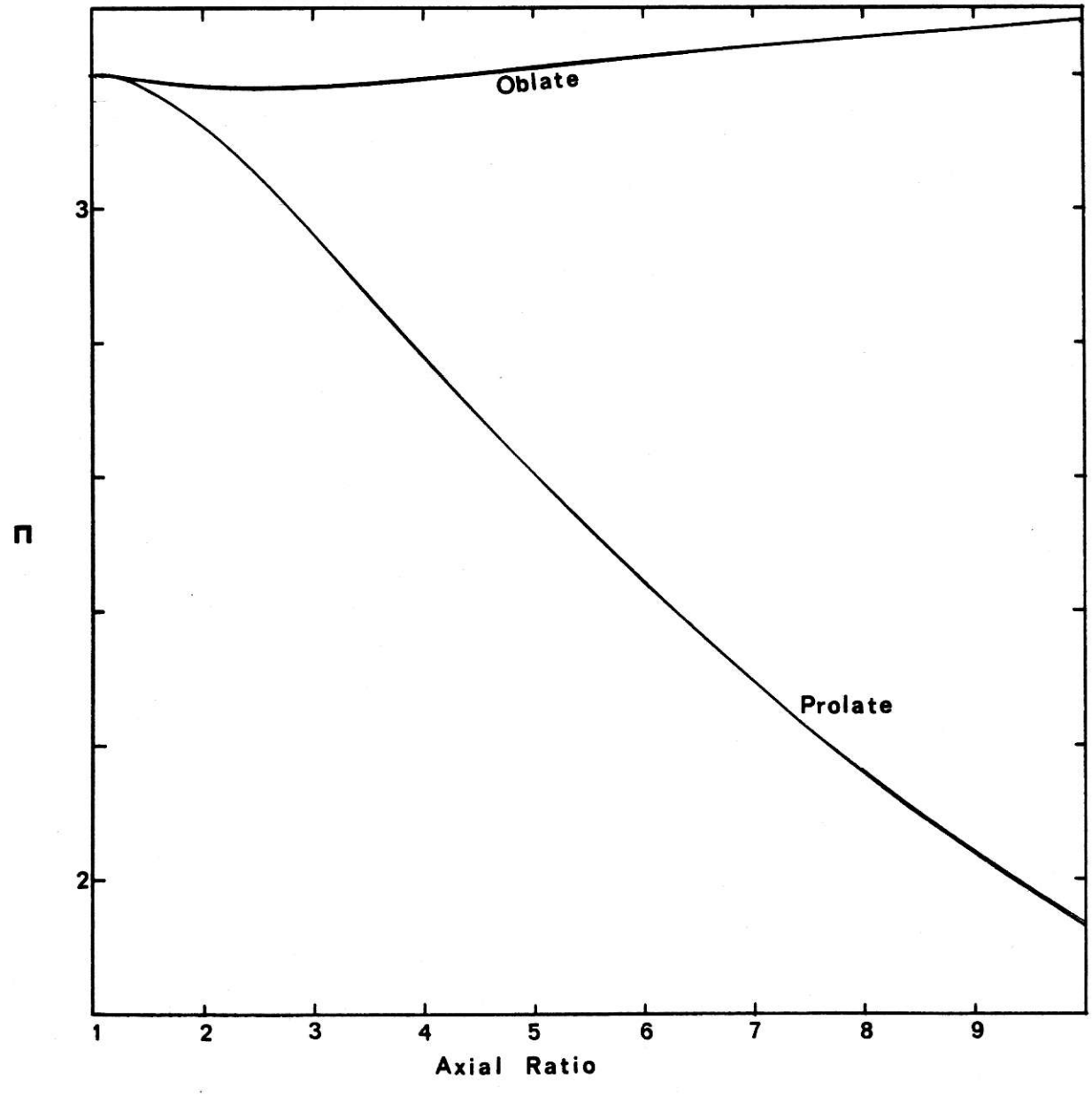

Figure 24. Plot of Π as a function of axial ratio for ellipsoids of revolution

BIBLIOGRAPHY.

Alexander, A.E. and Johnson, P. (1949)

'Colloid Science', Volume 2, Oxford University Press

Alpert, S.S. and Banks, G. (1976)

Biophysical Chem. 4, 287

Baghurst, P.A., Nichol, L.W., Ogston, A.G., Winzor, D.J. (1975)

Biochem. J. 147, 575

Ballinger, K.W.A. and Jennings, B.R. (1979)

Nature 282, 699

Batchelor, G.K. (1967)

'An Introduction to Fluid Mechanics', Cambridge University Press

Batchelor, G.K. (1970)

J. Fluid Mech. 41, 545

Batchelor, G.K. and Green, J.T. (1972)

J. Fluid Mech. 56, 375

Beeman, W.W., Koesberg, P., Anderegg, J.W. and Webb, M.B. (1957)

in 'Handbuck der Physik', (Flugge, S. ed.), 32, 321, Springer-Verlagg (Berlin)

Benoit, H. (1951)

Ann. Physik. 6, 561

Berne, P.J. and Pecora, R. (1974)

Ann. Rev. Phys. Chem. 25, 233

Blake, C.C.F. (1975)

Essays in Biochem. II, 37

Blake, C.C.F., Geisow, M.J. and Oatley, S.J. (1978)

J. Mol. Biol. 121, 339

Blake, C.C.F., Koenig, D.F., Mair, G.A., North, A.C.T., Phillips, D.C. and Sarma, V.R. (1965)

Nature 206, 757

Bloomfield, V.A., Dalton, W.O. and Van Holde, K.E. (1967)

Biopolymers 5, 135

Bresler and Talmud (1944)

CR Acad. Sci. URSS, 43, 310

Brinkman, H.C., Hermans, J.J., Oosterhoff, L.J., Overbeek, J. Th. G., Polder, D., Staverman, A.J. and Wiebenga, E.H. (1949)

Proc. Int. Rheol. Congress (Schveningen) II, 77

Brenner, H. (1970)

J. Coll. Int. Sci. 32, 141

Brenner, H. (1972a)

Chem. Eng. Sci. 27, 1069

Brenner, H. (1972b)

Progr. Heat and Mass Transfer 5, 93

Cantor, C.R. and Tao, T. (1971)

Proc. Nucl. Acid Res. 2, 31

Cerf, R. and Scheraga, H.A. (1952)

Chem. Revs. 51, 185

Chapman, P.F. (1913)

Phil. Mag. 25, 475

Cheng, P.Y. and Schachman, H.K. (1955)

J. Polymer Sci. 16, 19

Chu, B. (1974)

'Laser Light Scattering', Academic, New York

Chwang, A.T. (1975)

J. Fluid Mech. 72, 17

Clenshaw, C.W. and Curtis, A.R. (1960)

Num. Math. 2, 197

Creeth, J.M. and Knight, C.G. (1965)
Biochim. Biophys. Acta 102, 549

Cummings, H.Z. and Pike, E.R. (1973)
(eds.) 'Photon Correlation and Light Beating Spectroscopy', Plenum, New York

Dickerson, R.E. and Geiss, I. (1969)
'The Structure and Action of Proteins', Benjamin, California

Dougherty, J. and Kreiger, I.M. (1972)
in Kreiger, Adv. Colloid Sci. 3, 111

Edsall, J.T. (1953)
in 'The Proteins' (Neurath, H. and Bailey, K. eds) 1B, Chapter 7, Academic, New York

Edwardes, D. (1892)
Quart. J. Math. 26, 70

Einstein, A. (1905)
Ann. Physik 17, 549

Einstein, A. (1906)
Ann. Physik 34, 591

Einstein, A. (1911)
Ann Physik 34, 591

Emes, C.H. (1977)

Ph. D. thesis, University of Leicester

Emes, C.H. and Rowe, A.J. (1978a)

Biochim. Biophys. Acta 537, 110

Emes, C.H. and Rowe, A.J. (1978b)

Biochim. Biophys. Acta 537, 125

Farrant, J.L. (1954)

Biochim. Biophys. Acta 13, 569

Feldman, R.J. (1976)

'Atlas of Macromolecular Structure on Microfiche', Traco Jitco Int., Rockville, Md. USA

Gans, R. (1928)

Ann. Physik 86, 628

Garcia Bernal, J.M. and Garcia de la Torre, J. (1980)

Biopolymers 19, 628

Garcia de la Torre, J. and Bloomfield, V.A. (1977a)

Biopolymers 16, 1747

Garcia de la Torre, J. and Bloomfield, V.A. (1977b)

Biopolymers 16, 1765

Garcia de la Torre, J. and Bloomfield, V.A. (1977c)

Biopolymers 16, 1779

Garcia de la Torre, J. and Bloomfield, V.A. (1978)

Biopolymers 17, 1605

Gardner, D.G., Gardner, J.C., Laush, G. and Meinke, W.W. (1959)

J. Chem. Phys. 31, 978

Giesekus, H. (1962)

Rheol. Acta 2, 50

Gill, P.E. and Murray, W. (1976)

Nat. Phys. Lab. report NAC 72

Gold, O. (1937)

Ph. D. thesis, University of Vienna

Goodwin, J.W. (1975)

Colloid Science 2 (Chemical Society), 246

Guoy, L.G. (1910)

J. Phys. Chem. 9, 457

Hall, C.E. and Slayter, H.S. (1959)

J. Biophys. Cytol. 5, 11

Harding, S.E. (1980a)

Biochem. J. 189 (in press)

Harding, S.E. (1980b)

mss. submitted to J. Phys. Chem.

Harrison, P.M. (1959)

J. Mol. Biol. 1, 69

Herzog, R.O., Illig, R. and Kudar, H. (1934)

Z. Phys. Chem. A167, 329

Holtzer, A. and Lowey, S. (1956)

J. Am. Chem. Soc. 78, 5954

Jablonski, A. (1961)

Naturforsch 169, 1

Jeffrey, G.B. (1922)

Proc. Roy. Soc. (London) A102, 476

Johnson, P. and Mihalyi, E. (1965)

Biochim. Biophys. Acta 102, 476

Jost, J.W. and O'Konski, C.T. (1978)

in 'Molecular Electro Optics' (O'Konski, C.T. ed.) Volume 2, 529

Kartha, G., Bello, J. and Harker, D. (1967)

Nature 213, 862

Kendrew, J.C., Bodo, G., Dintzis, H.M., Parrish, R.G., Wycoff, H. and Phillips, D.C. (1958)

Nature 181, 665

Kim, S.H. (1974)

in 'Biochemistry' (Stryer, L.) 653, Freeman, San Francisco

Kirkwood, J.G. (1967)

'Macromolecules' (Aueur, P.L. ed.), Gordon and Breach

Koenig, S.H. (1975)

Biopolymers 14, 2421

Kratky, O., Leopold, H. and Stabinger, H. (1969)

Z. Angew. Phys. 27, 273

Kratky, O., Leopold, H. and Stabinger, H. (1969)

in 'Methods in Enzymology' (Hirs, C.H.W. and Timasheff, S.N. eds.), 27, 98, Academic, London

Krause, S. and O'Konski, C.T. (1959)

J. Am. Chem. Soc. 81, 5082

Kuff, E.J. and Dalton, A.L. (1957)

J. Ultrastructure Res. 1, 62

Kuhn, W. and Kuhn, H. (1945)

Helvetica Chimica Acta 38, 97

Kynch, G.J. (1956)

Proc. Roy. Soc. (London) A237, 90

Labaw, L.W. and Wycoff, R.W.G. (1957)

Biochim. Biophys. Acta 25, 263

Lauffer, M.A. (1942)

Chem. Rev. 31, 561

Laurent, T.C. and Killander, J. (1964)

J. Chromatog. 14, 317

Lipscomb, W.N. (1971)

Proc. Robert A. Welch Found. Conf. Chem. Res. 15, 134

Lloyd, P.H. (1974)

'Optical Methods in Ultracentrifugation, Electrophoresis and Diffusion',

Clarendon Press, Oxford

Lucas, C.W. and Terrill, C.W. (1970)

Collected Algorithms from CACM, No. 404

Manley, R. and Mason, S. G. (1954)

Canad. J. Chem. 32, 763

Martin, R.B. (1964)

'Introduction to Biophysical Chemistry' Chap. 11, McGraw-Hill, New York

McCammon, J.A., Deutch, J.M. and Bloomfield, V.A. (1975)

Biopolymers 14, 2479

Mehl, J.W., Oncley, J.L. and Simha, R. (1940)

Science 92, 132

Mendelson, R. and Hartt, J. (1980)

EMBO Workshop on Muscle Contraction, Alpbach Conf. Austria

Mihalyi, E. and Godfrey, J. (1963)

Biochim. Biophys. Acta 67, 90

Memming, R. (1961)

Z. Physik. Chem. (Frankfurt) 28, 169

Mooney, M. (1951)

J. Coll. Sci. 6, 162

Mooney, M. (1957)

J. Coll. Sci. 12, 575

Munro, I., Pecht, I. and Stryer, L. (1979)

Proc. Nat. Acad. Sci. (USA) 76, 56

Nichol, L.W., Jeffrey, P.D., Turner, D.R. and Winzor, D.J. (1977)

J. Phys. Chem. 81, 776

Nisihara, T. and Doty, P. (1958)

Proc. Nat. Acad. Sci. (USA) 44, 411

Oberbeck, A. (1876)

J. reine. angew. Math. 81, 62

O'Connor, D.V., Ware, W.R. and Andre, J.C. (1979)

J. Phys. Chem. 83, 1333

Offer, G., Moos, C. and Starr, R. (1973)

J. Mol. Biol. 74, 653

O'Hara and Smith (1968)

Comp. Journal 11, 213

O'Konski, C.T. and Haltner, A.J. (1956)

J. Am. Chem. Soc. 78, 3604

Oliver, J. (1972)

Comp. Journal 15, 141

Oncley, J.L. (1940)

J. Phys. Chem. 44, 1103

Oncley, J.L. (1941)

Ann. New York Acad. Sci. 41, 121

Paradine, C.G. and Rivett, B.H.P. (1960)

'Statistical Methods for Technologists', English Universities Press, London

Pearce, T.C., Rowe, A.J. and Turnock, G. (1975)

J. Mol. Biol. 97, 193

Perrin, F. (1934)

J. Phys. Radium 5, 497

Perrin, F. (1936)

J. Phys. Radium 7, 1

Perutz, M.F., Rossmann, M.G., Cullis, A.F., Muirhead, H., Will, G. and North, A.C.T. (1960)

Nature 185, 416

Powell, D.R. and MacDonald, J.R. (1972)

Comp. Journal 15, 148

Pytkowickz, R.M. and O'Konski, C.T. (1959)

J. Am. Chem. Soc. 81, 5082

Rallison, J.M. (1978)

J. Fluid Mech. 84, 237

Riddiford, C.L. and Jennings, B.R. (1967)

Biopolymers 5, 757

Ridgeway, D. (1966)

J. Am. Chem. Soc. 88, 1104

Ridgeway, D. (1968)

J. Am. Chem. Soc. 90, 18

Rowe, A.J. (1977)

Biopolymers 16, 2595

Rowe, A.J. (1978)

Techniques in Protein and Enzyme Biochem. B105a, 1

Saito, N. (1951)

J. Phys. Soc. (Japan) 6, 297

Scheraga, H.A. (1955)

J. Chem. Phys. 23, 1526

Scheraga, H.A. (1961)

'Protein Structure', Academic, New York

Scheraga, H.A. and Mandelkern, L. (1953)

J. Am. Chem. Soc. 79, 179

Simha, R. (1940)

J. Phys. Chem. 44, 25

Simha, R. (1952)

J. Appl. Phys. 23, 1020

Shaw, D.J. (1970)

'Introduction to Colloid and Surface Chemistry' (2nd edn.), Butterworths

Small, E.W. and Isenberg, I. (1977)

Biopolymers 16, 1907

Sorenson, N.A. (1930)

CR Lab. Carlsberg 18, No. 5

Squire, P.G. (1970)

Biochim. Biophys. Acta 221, 425

Squire, P.G. (1978)

in 'Molecular Electro Optics' (O'Konski, C.T. ed.) Volume 2, 565

Squire, P.G., Moser, L. and O'Konski, C.T. (1968)

Biochemistry 7, 4261

Stacey, K.A. (1956)

'Light Scattering in Physical Chemistry', Butterworths, London

Stokes, Sir G. (1851)

Trans. Cambridge Phil. Soc. 9, 8

Stokes, Sir G. (1880)

'Mathematical and Physical Papers', Cambridge University Press

Svedberg, T. and Pedersen, K.O. (1940)

'The Ultracentrifuge', Oxford University Press

Tanford, C. (1955)

J. Phys. Chem. 59, 798

Tanford, C. (1961)

'Physical Chemistry of Macromolecules', Wiley, New York

Theorell, H. (1934)

Biochem. Z. 268, 46

Vand, V. (1948)

J. Phys. Coll. Chem. 52, 277

Van de Hulst, H.C. (1957)

'Light Scattering by Small Particles', Wiley, New York

Van Holde, K.E. (1971)

'Physical Biochemistry', Prentice Hall, New Jersey

Wahl, P. (1966)

Compt. Rend. Acad. Sci. (Paris) 263D 1525

Wales, M. and Van Holde, K.E. (1954)

J. Polymer Sci. 14, 81

Wilde, D.J. (1964)

'Optimum Seeking Methods', Prentice Hall, New Jersey

Williams, R.C., Ham, W.T. and Wright, A.K. (1976)

Anal. Biochem. 73, 52

Wilson, R.W. and Bloomfield, V.A. (1979a)

Biopolymers 18, 1205

Wilson, R.W. and Bloomfield, V.A. (1979b)

Biopolymers 18, 1543

Yang, J.T. (1961)

Adv. Protein Chem. 16, 323

Zimm, B.H. (1948)

J. Chem. Phys. 16, 1093

Zimm, B.H. (1956)

J. Chem. Phys. 24, 269